
Pergamon
www.elsevier.com/locate/pnucene

Available online at www.sciencedirect.com
SCIENCE DIRECT®

Progress in Nuclear Energy, Vol. 42, No. 1, pp. 55–106, 2003
Published by Elsevier Science Ltd
Printed in Great Britain
0149-1970/03/$ - see front matter

PII: S0149-1970(02)00098-7

Analytical Benchmark Test Set For Criticality Code Verification

Avneet Sood, R. Arthur Forster, and D. Kent Parsons

Los Alamos National Laboratory, Applied Physics (X) Division, X-5 Diagnostics Applications Group, P.O. Box 1663, MS F663, Los Alamos, NM 87545

Abstract

A number of published numerical solutions to analytic eigenvalue (k_{eff}) and eigenfunction equations are summarized for the purpose of creating a criticality verification benchmark test set. The 75-problem test set allows the user to verify the correctness of a criticality code for infinite medium and simple geometries in one-, two-, three-, and six-energy groups, with one-, two-, and four-media. The problems include both isotropic and linearly and quadratically anisotropic neutron scattering. The problem specifications will produce both k_{eff}=1 and the quoted k_{∞} to at least five decimal places. MCNP (Briesmeister, 1997) and DANTSYS (Alcouff, R.E, et al., 1995) have been verified using these problems. Additional uses of the test set for code verification are also discussed. Published by Elsevier Science Ltd.

Key words: analytic; benchmark; criticality; code verification

1 Introduction

This paper describes a set of benchmark problems with analytic eigenvalue (k_{eff}) and eigenfunction (flux) solutions to the neutron transport equation from peer-reviewed journal articles. The purpose of the test set is to verify that transport algorithms and codes can correctly calculate the analytic k_{eff} and fluxes. The authors believe the reported eigenvalues and eigenfunctions to be accurate to at least five decimal places even though many references often report higher precision values. The higher precision eigenvalues and eigenfunctions from the references are reproduced here. These test set problems for infinite medium, slab, cylindrical, and spherical geometries in one- and

Email addresses: asood@lanl.gov (Avneet Sood), raf@lanl.gov (R. Arthur Forster), dkp@lanl.gov (D. Kent Parsons).

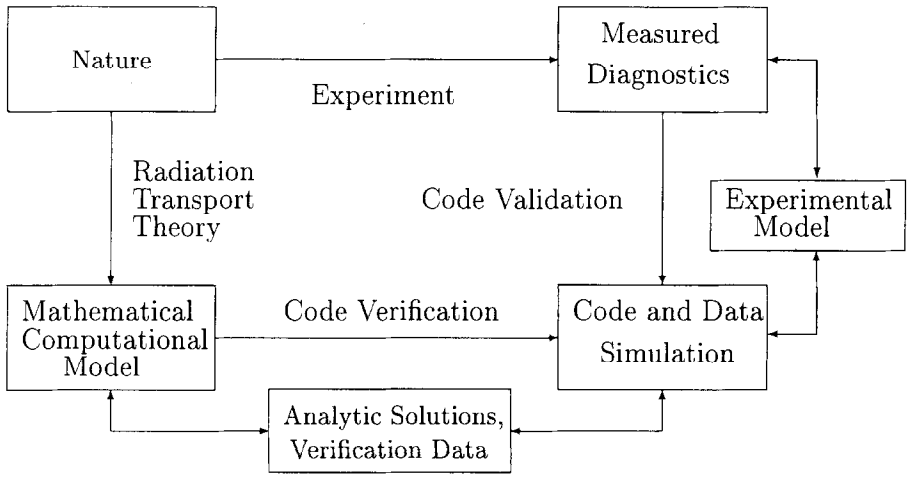

Fig. 1. A Personal View of Computer Simulation of Radiation Transport

two-energy groups, with one-, two-, and four-media, and isotropic and both linearly and quadratically anisotropic scattering are completely described using the listed references in this paper. A three-group infinite medium and a six-group variant k_∞ problem (unpublished) are also included. This paper includes updates and minor corrections to previous Los Alamos papers and reports.[3],[4],[5],[6]

1.1 Verification and Validation

Verification is defined as "the process of evaluating a system or component to determine whether the products of a given development phase satisfy the conditions imposed at the start of the phase"[7] or as a proof of correctness. **Confirmation (proof) of correctness** is defined as "a formal technique used to prove mathematically that a computer program satisfies its specified requirements."[7] In contrast to verification, **validation** is "the process of evaluating a system or component during or at the end of the development process to determine whether it satisfies specified requirements."[7] Thus code verification checks that the implemented code precisely reflects the intended calculations and that these calculations have been executed correctly. Code validation compares the accuracy of these calculated results usually with experimental data.

Figure 1 summarizes the process of modeling nature to developing a computer code simulation of radiation transport.[8] One path to simulating radiation transport is to develop a theoretical physics model and describe it with math-

ematical equations. Exact solutions to these complex theoretical equations are often impossible. Solutions to the mathematical equations require simplifying assumptions and are approximated with a carefully developed computer code. Code verification is the link between these mathematical and computational equations and the computer simulation. Verification of the code and data simulation includes comparisons of calculated results with analytic solutions and simplified verification data intended to be used only to verify computer code numerical performance. Other forms of code verification include comparisons with an accepted standard set of code output for regression testing, results from other computer codes, and line-by-line debugging.

A second path to characterizing radiation transport is to perform careful experiments and measure physical quantities using diagnostics. The accuracy of the measured diagnostics is limited by approximations and assumptions in the experimental methods and by the precision of the diagnostic equipment. Carefully designed experiments often infer or directly measure a desired physical parameter from the theoretical models and equations and thus are measurements of its true value. Code validation is the link between the measured diagnostics and the computer code with the general purpose physical data required by the computer simulation. Code and data validation includes comparison of the calculated code output with results from experiments and from other computer codes.

Figure 1 shows the process of developing a computer code simulation requires code verification, validation, and physical data. Importantly, the figure shows there is no direct path linking nature and computer simulation. Code verification must be performed before code validation. The objectives of this paper are to define and document a set of analytic eigenvalue and eigenfunction benchmarks for verifying criticality codes. **Benchmark** is defined as "a standard against which measurement or comparisons can be made."[7] Available benchmarks for code verification do not focus on criticality problems.[9] Validation benchmarks from critical experiments do exist, but are not verification benchmarks.[10] An initial effort to compile a benchmark test set for criticality calculation verification was begun, but not completed.[11],[12] The analytic benchmarks described here can be used to verify computed numerical solutions for k_{eff} and the associated flux with virtually no uncertainty in the numerical benchmark values.

1.2 Why These Solutions Serve as a Test Set

All critical dimensions, k_{eff}, and scalar neutron flux results quoted here are based on numerical computations using the analytic solutions to the k_{eff} eigenvalue (homogeneous) transport equation for "simple" problems. The analytic

methods used include Case's singular eigenfunction[13], F_N and S_N methods, [14],[15] and Green's functions.[16]

All of these test set problem specifications and results are from peer-reviewed journals, and have, in some cases, been solved numerically using more than one analytic solution. All calculated values for critical dimensions, k_{eff}, and the scalar neutron flux are believed to be accurate to at least five decimal places. Several critical dimensions and scalar neutron flux are reported to more than five decimal places. The higher precision eigenvalues and eigenfunctions from the references are simply reproduced here.

1.3 Scope of the Criticality Verification Test Set

The verification test set was chosen to represent a "wide" range of problems from the relatively small number of published solutions. These problems include simple geometries, few neutron energy groups, and simplified (isotropic and linearly anisotropic) scattering models. The problems use neutron cross sections that are reasonable representations of the materials described. These cross sections are **not** general purpose multi-group values. The cross sections are used because they are extracted from the literature results and are intended to be used only to verify algorithm performance and **not** to predict criticality experiments.

The basic geometries include an infinite medium, slab, cylinder, and sphere with one- and two-energy group representations of uniform homogeneous materials. The slab and cylinder geometries are one-dimensional, as shown in Figure 2; that is, each is finite in one dimension (thickness for slab and radius for the cylinders) and infinite elsewhere. The two-media problems surround each geometry with a specified thickness of reflector. Solutions for one-, two-, and three-group infinite medium problems are derived in Appendix A.

The emphasis of the test set is on the fundamental eigenvalue, k_{eff}. All k_{eff} eigenvalues for finite fissile materials are unity to at least five decimal places. The k_∞ values for a uniform homogeneous infinite medium are greater than unity. Few numerical eigenfunction solutions are published; consequently, mainly one-group and uniform homogeneous infinite medium fluxes are included in the test set results.

The critical dimension, r_c, is defined pictorially for the one-dimensional, one-medium problem geometries in Figure 2, as well as the two-media infinite slab lattice cell. Reflector dimension(s) are provided for the reflected cases.

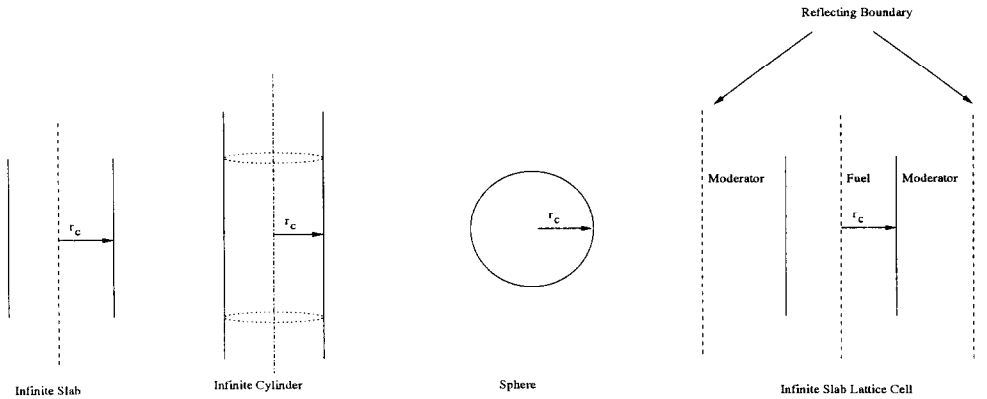

Fig. 2. Critical Dimension, r_c, for Bare One-Dimensional Geometries and Infinite Slab Lattice Cell

To assist in verification, each problem has a unique identifier. Since the test set includes bare and multi-media problems, there are two forms of the identifier. The first form is for a bare geometry:

Fissile Material - Energy Groups - Scattering - Geometry

The possible entries for each category are listed in Table 1. The fissile materials and identifier consist of Pu-239 (PU), U-235 (U), highly enriched uranium-aluminum-water assembly (UAL), low enrichment uranium and D_2O reactor system (UD2O), and a highly enriched uranium research reactor (URR). The identifier may be followed by a letter to differentiate between different cross section sets from nominally the same material. The table lists identifiers for the reflector material (if any), number of energy groups, scattering order, and geometry. The geometry is identified by the first two letters in the table. The exception is for the infinite slab lattice cell which uses ISLC. An example of the one material form of the identifier is:

U-2-0-SP

which is the identifier for a bare U-235 reactor (no reflector), 2 energy groups, isotropically scattering, in spherical geometry.

The second form of the identifier includes the reflecting material. The reflectors are usually H_2O with an exception of a three region Fe, Pb, Fe reflector. Although many of the reflectors are identified as H_2O, the reflector cross sections are unique to each problem. Consequently, a letter may follow H2O indicating the H_2O cross section set used. The multi-media identifier form is:

Fissile Material - Reflecting Material (thickness) - Energy Groups - Scattering - Geometry

To separate multiple reflector thicknesses for the same fissile material, the

Table 1
Nomenclature for Problem Identifiers

Fissile Material	Reflector Material	Energy Groups	Scattering Order	Geometry
PU	bare	1 group	0 - P_0 Isotropic	INfinite
U	H2O	2 groups	1 - P_1 Anisotropic	SLab
UD2O	Fe-Na	3 groups	2 - P_2 Anisotropic	CYlinder
UAL		6 groups		SPhere
URR				Infinite Slab Lattice Cell

thickness is given in parenthesis in the title in units of mean free paths (mfp). For example,

UD2O-H2O(10)-1-0-SL

is the identifier for a uranium and D_2O reactor with a H_2O reflector of 10 mean free path thickness, one-energy group, isotropically scattering, in slab geometry. An "IN" in parenthesis after the H2O means an infinite water reflector.

There are 43 problems in the one-energy group case; 30 problems assume isotropic scattering and 13 have anisotropic scattering. For the two-energy group problems, there are 30 problems subdivided into 26 isotropic scattering problems and 4 linearly anisotropic problems. Also included for an infinite medium are a three-group and a six-group (2 coupled sets of three groups) isotropic problem. The test set includes 24 infinite medium problems, 24 slabs, 9 one-energy group cylinders, 14 spheres, and 4 infinite slab lattice cells.

2 Uses of the Criticality Verification Test Set

This paper provides all necessary problem definitions and published critical dimensions, k_{eff}, and scalar neutron flux results to verify a criticality transport algorithm or code and associated numerics such as random number generation and round-off errors. All material cross sections provided are macroscopic, so the atom density used by the code should be unity. Cross section values are assumed accurate to the number of decimal places reported. Not all of the analytic solutions from the references are used, however, because the number of problems in the test set becomes too large. For other solutions not included in this paper, see the reference list.

The verification test set problems can be used in several ways. The user can choose to simply calculate the problems and compare forward and adjoint

k_{eff} and neutron flux results with the benchmark solutions. However, there are several more verification processes that could be included. For example, in Monte Carlo codes, examining two forms of cross sections representation we might include multi-group and pointwise representation of multi-group data. In multi-group problems, an alternative verification procedure is to change the energy group structure when up-scattering is allowed; that is, reverse the order of the fast and slow groups.

Another part of code verification is testing different representations of the same geometry (e.g. reflecting boundaries and lattices). An example is an infinite one-dimensional slab (finite in one dimension and infinite in the other two dimensions) as shown in Figure 2, which could be modeled as a three-dimensional cube with four reflective boundaries. Other geometry options can be tested by constructing several smaller cubes inside of the three-dimensional representation of a one-dimensional critical slab. The infinite medium problem can be represented by using large geometric boundaries, reflecting boundaries, or infinite lattices of finite shapes. Infinite medium problems can be used to verify constant scalar and angular flux in each energy group as well as scalar flux ratios for more than one energy group. Three-dimensional geometric representations of optically small objects can also be tested for k_∞ in infinite medium problems.[17] Purely absorbing one-group infinite medium problems can provide faster code verification since scattering does not alter the infinite medium k_∞ (see Appendix A).

Another use of this verification test set includes testing of any flux approximations. This can be especially important at near tangential angles where many codes assume a value for the incident angle. This can also affect k_{eff} if it is estimated by same section of code that calculates the flux.

Different calculation capabilities of a code should be tested using these problems. For Monte Carlo codes, different variance reduction methods such as analog or implicit capture and geometric splitting or Russian roulette can be verified. Cycle-to-cycle correlations in the estimated k_{eff} standard deviation must be taken into account to form valid k_{eff} confidence intervals. Statistically independent runs can be made and analyzed if necessary. The magnitude of any negative bias in k_{eff}, which is a function of the number of neutron histories per fission generation, also needs to be considered and made smaller than 0.00001. [18]

Deterministic codes can assess convergence characteristics and correctness of k_{eff} and the flux as a function of space and angle representation. Various characteristics of discrete ordinates numerics can also be checked such as the effects of eigenvalue search algorithms, angular redistribution terms in curvilinear geometries, ray effects, and various alternative geometric descriptions.

3 Neutron Transport Equation Overview

The neutron transport equation being solved in these benchmark problems is briefly described for one- and two-energy groups and the isotropic and linearly anisotropic cases. The infinite medium solutions for k_∞ and the flux ratios are described in Appendix A.

3.1 General k_{eff} Eigenvalue Equation

The steady state neutron transport equation can be written as a k_{eff} eigenvalue problem as: [19]

$$\vec{\Omega}\cdot\nabla\Psi(\vec{r},E,\vec{\Omega})+\Sigma_t(\vec{r},E)\Psi(\vec{r},E,\vec{\Omega})=\int_0^\infty dE'\int_{4\pi}d\vec{\Omega}'\Sigma_s(\vec{r},E'\to E,\vec{\Omega}'\to\vec{\Omega})\Psi(\vec{r},E',\vec{\Omega}')$$
$$+\chi(E)\int_0^\infty dE'\frac{\nu(\vec{r},E')}{4\pi k_{eff}}\Sigma_f(\vec{r},E')\int_{4\pi}\Psi(\vec{r},E',\vec{\Omega}')d\vec{\Omega}' \tag{1}$$

where:

$\Psi(\vec{r},E,\vec{\Omega})$ = angular neutron flux as a function of space $\vec{r}$, energy E, and angle $\vec{\Omega}$

$\Sigma_t(\vec{r},E)$ = total neutron macroscopic cross section

$\Sigma_s(\vec{r},E'\to E,\vec{\Omega}'\to\vec{\Omega})dEd\vec{\Omega}$ = neutron scattering macroscopic cross section from E' to $E+dE$ in direction $d\vec{\Omega}'$ about $\vec{\Omega}$

$= \Sigma_{elastic}+\Sigma_{(n,n')}+2\Sigma_{(n,2n)}+\ldots$

$\Sigma_f(\vec{r},E')$ = neutron fission macroscopic cross section

$\nu(\vec{r},E')$ = number of neutrons emitted from each fission event

$\chi(E)$ = fission neutron energy distribution

For these test problems, there are no (n,xn') reactions, $x>1$, included in Σ_s. Therefore, $\Sigma_c=\Sigma_t-\Sigma_s-\Sigma_f$, where Σ_c is the neutron capture cross section (zero neutrons emitted). This paper also provides values for the scalar neutron flux, which is defined as $\phi(r,E)=\int_\Omega\Psi(\vec{r},E,\vec{\Omega})d\vec{\Omega}$. The reported scalar neutron flux values are normalized to the flux at the center of the fissile material.

The k_{eff} eigenvalue is only associated with the fission reaction and no other multiplying process such as $(n, 2n)$. The fundamental eigenvalue, k_{eff}, is unity for a critical system, less than unity for a subcritical system, and greater than unity for a supercritical system. The steady state k_{eff} eigenvalue equation is physically correct only when k_{eff} is unity and there is no decay or growth in $\Psi(r, E, \vec{\Omega})$. A solution when k_{eff} is not unity is still a valuable indicator of the ability of a system to sustain a fission chain reaction. When an infinite medium is considered, k_{eff} will be referred to as k_∞. This paper gives results for the fundamental eigenvalue. For higher eigenvalue results see references [20], [21], [22], [24], [25], [26], [27].

3.2 One-Energy Group in One-Dimensional Slab Geometry

3.2.1 Isotropic Scattering.

The one-energy group, homogeneous medium with isotropic scattering transport equation for a slab can be written in terms of an optical thickness $(z = \Sigma_t x)$ as: [19]

$$\mu \frac{\partial \Psi(z,\mu)}{\partial z} + \Psi(z,\mu) = \frac{c}{2} \int_{-1}^{1} \Psi(z,\mu') d\mu' \tag{2}$$

where:

$$c = \frac{\Sigma_s + \frac{\nu \Sigma_f}{k_{eff}}}{\Sigma_t} \tag{3}$$

The eigenvalue form of c is defined as the mean number of secondary neutrons produced per neutron reaction and is also known as the secondaries ratio. This equation still requires elaborate mathematics to solve as reported in the literature. Derivation of the one-energy group k_∞ solution for the infinite medium case is shown in Appendix A.

The literature uses this form of the neutron transport equation with a non-reentrant boundary condition to derive one-energy group, isotropic scattering analytic solutions for the critical (k_{eff}=1) dimensional scalar neutron flux. It should be noted that c values for $k_{eff} = 1$ in equation 3 are presented in the literature, thereby making $c = \frac{\Sigma_s + \nu \Sigma_f}{\Sigma_t}$. The typical range of c found in the literature for fissile materials is from 1.01 to 2.00. The one-group cross sections selected for the test set mimic the physical characteristics of the two-group problems and range from 1.02 to 1.50. A value of c of 1.5 is the upper limit for real fissile materials.

3.2.2 *Linearly Anisotropic Scattering.*

The scattering term, $\Sigma_s(\vec{r}, E' \rightarrow E, \vec{\Omega}' \rightarrow \vec{\Omega})$ can be a strong function of the cosine of the scattering angle, $\mu_0 = \vec{\Omega}' \cdot \vec{\Omega}$. The angular dependence can be analyzed by Legendre polynomial series expansion of $\Sigma_s(\vec{r}, E' \rightarrow E, \vec{\Omega}' \cdot \vec{\Omega})$.[28] Using the Legendre polynomial expansion, the one-energy group, one-dimensional slab, neutron transport equation can be written in a similar form to equation 2:[29],[30]

$$\mu \frac{\partial \Psi(z,\mu)}{\partial z} + \Psi(z,\mu) = \frac{c}{2} \int_{-1}^{1} \Psi(z,\mu')(1 + \mu'\mu) d\mu'$$

This form of the neutron transport equation is often found in the literature. The solution of this equation includes linearly anisotropic scattering; however, it also includes a linearly anisotropic fission source emission. For problems that include the anisotropic effect on the fission term, see references [22], [29], [30]. Numerical solutions exist that do not force the anisotropic effect on the fission term. This limitation on the different anisotropic behavior of scattering and fission can be removed by using different transfer functions for scattering and fission. [31] Solutions for the higher eigenvalues exist for this form of the transport equation.[20],[21],[22],[24],[25],[26],[27]

3.3 *Two-Energy Groups in One-Dimensional Slab Geometry*

3.3.1 *Isotropic Scattering.*

Using the same procedures as in the one-group case, the two-energy group form of the transport equation for a slab can be written as: [15]

$$\mu \frac{\partial \Psi_1(x,\mu)}{\partial x} + \Sigma_1 \Psi_1(x,\mu) = \frac{\Sigma_{11}}{2} \int_{-1}^{1} \Psi_1(x,\mu') d\mu' + \frac{\Sigma_{12}}{2} \int_{-1}^{1} \Psi_2(x,\mu') d\mu' \tag{4}$$

$$\mu \frac{\partial \Psi_2(x,\mu)}{\partial x} + \Sigma_2 \Psi_2(x,\mu) = \frac{\Sigma_{21}}{2} \int_{-1}^{1} \Psi_1(x,\mu') d\mu' + \frac{\Sigma_{22}}{2} \int_{-1}^{1} \Psi_2(x,\mu') d\mu' \tag{5}$$

where:

Σ_i = total neutron macroscopic cross section of group i

Σ_{ij} = total neutron group transfer macroscopic cross section from group j to group i

In this paper, the fast energy group is group 2 to be consistent with most of the references. This notation is the reverse of most nuclear engineering textbooks.

Assuming group 2 is the fast group and no non-fission up-scatter for the slow group 1, the group transfer cross sections are given by:

$$\Sigma_{11} = \Sigma_{11s} + \chi_1 \nu_1 \Sigma_{1f}/\mathrm{k}_{eff}$$
$$\Sigma_{21} = \chi_2 \nu_1 \Sigma_{1f}/\mathrm{k}_{eff}$$
$$\Sigma_{12} = \Sigma_{12s} + \chi_1 \nu_2 \Sigma_{2f}/\mathrm{k}_{eff}$$
$$\Sigma_{22} = \Sigma_{22s} + \chi_2 \nu_2 \Sigma_{2f}/\mathrm{k}_{eff}$$

Note that $\Sigma_i = \Sigma_{ic} + \Sigma_{if} + \Sigma_{iis} + \Sigma_{jis}$, where the Σ_{jis} represents nonfission scattering to group $j \neq i$. This equation for Σ_i again assumes that the $\Sigma_{(n,2n)_i}$ + ... components are zero.

The two-energy group form of the transport equation, which has solutions in the literature, can be written in a similar form to the one-group equations utilizing the optical thickness parameter, $z = \Sigma_2 x$, but in matrix-vector notation as seen below.

$$\mu \frac{\partial \bar{\Psi}(z,\mu)}{\partial z} + \bar{\bar{\Sigma}} \bar{\Psi}(z,\mu) = \frac{\bar{\bar{C}}}{2} \int_{-1}^{1} \bar{\Psi}(z,\mu') d\mu' \tag{6}$$

where:

$$\bar{\Psi}(z,\mu) = \begin{bmatrix} \Psi_1(z,\mu) \\ \Psi_2(z,\mu) \end{bmatrix}, \bar{\bar{\Sigma}} = \begin{bmatrix} \Sigma & 0 \\ 0 & 1 \end{bmatrix}, \bar{\bar{C}} = \begin{bmatrix} c_{11} & c_{12} \\ c_{21} & c_{22} \end{bmatrix} \tag{7}$$

and

$$c_{ij} = \Sigma_{ij}/\Sigma_2. \tag{8}$$

The derivations for the infinite medium k_∞ and the group 2 to group 1 flux ratio are given in Appendix A.

3.3.2 Linearly Anisotropic Scattering.

One of the above simplifying assumptions to the steady state neutron transport equation is that neutron scattering is isotropic (no angular dependence). However, the scattering term, $\Sigma_s(\vec{r}, E' \rightarrow E, \vec{\Omega}' \rightarrow \vec{\Omega})$ can be a strong function of the cosine of the scattering angle, $\mu_0 = \vec{\Omega}' \cdot \vec{\Omega}$. This angular dependence can be analyzed by Legendre polynomial series expansion of $\Sigma_s(\vec{r}, E' \rightarrow E, \vec{\Omega}' \cdot \vec{\Omega})$ [28], giving

$$\Sigma_s(\vec{r}, E' \rightarrow E, \vec{\Omega}' \cdot \vec{\Omega}) = \sum_{l=0}^{M} \frac{2l+1}{4\pi} \Sigma_{sl}(\vec{r}, E' \rightarrow E) P_l(\vec{\Omega}' \cdot \vec{\Omega}) \tag{9}$$

where M indicates the degree of anisotropy. For $M = 0$, scattering in the lab system is isotropic and for $M = 1$, scattering is linearly anisotropic. A complete mathematical description is in reference [19] and [28]. For linearly anisotropic scattering, the scattering cross section for general anisotropic scattering consists of two components, Σ_{s_0} and Σ_{s_1}, where Σ_{s_1} is the linear anisotropic scattering component and affects the scattering angular distribution for both in and out of group scattering. Anisotropic scattering can be forward or backward peaked and thus Σ_{s_1} can be positive or negative. The total scattering cross section is not dependent on Σ_{s_1}. The anisotropic cross section only affects the angular distribution. Infinite medium k_∞ and neutron flux results are independent of the anisotropic cross section.

Following the same procedures, the general two-speed linearly anisotropically scattering analogue to equation 6 which also has numerical solutions is:[32]

$$\mu \frac{\partial \bar{\Psi}(z,\mu)}{\partial z} + \bar{\bar{\Sigma}} \bar{\Psi}(z,\mu) = \frac{1}{2} \sum_{l=0}^{1} \bar{\bar{C}}_l P_l(\mu) \int_{-1}^{1} \bar{\Psi}(z,\mu') P_l(\mu') d\mu' \tag{10}$$

where:

$$\bar{\Psi}(z,\mu) = \begin{bmatrix} \Psi_1(z,\mu) \\ \Psi_2(z,\mu) \end{bmatrix}, \bar{\bar{\Sigma}} = \begin{bmatrix} \Sigma & 0 \\ 0 & 1 \end{bmatrix}, \bar{\bar{C}}_l = \begin{bmatrix} c_{11l} & c_{12l} \\ c_{21l} & c_{22l} \end{bmatrix} \tag{11}$$

and

$$c_{ijl} = (2l+1)\Sigma_{ijl}/\Sigma_2. \tag{12}$$

The Σ_{ijs_l} term is the linearly anisotropic scattering cross section and is given

in the problem descriptions without the $(2l + 1)$ term.

4 One-Energy Group Problem Definitions and Results

For the one-energy group cases, the critical dimension(s) for each geometry depends upon the c value chosen from the literature and not specific cross section sets. To use the literature results, the cross sections were selected to match published c values with k_{eff}=1 at low, middle, and high c values listed. Values ranging from 1.02, 1.30, 1.40, and 1.50 were chosen because they are similar to the physical systems in the two-group cases: uranium-D_2O reactor, U-235, and Pu-239. These problems use cross sections that are reasonable representations of these materials; however, these cross sections are **not** general purpose one-group values. The cross sections are used because they define the c values used in the literature and are intended to be used only to verify algorithm performance and **not** to predict any actual criticality experiments. Cross section values are assumed accurate to the number of decimal places reported.

The isotropic neutron macroscopic cross sections provided for each case are: the total cross section, Σ_t, the capture (no neutrons emitted) cross section, Σ_c, the scattering cross section, Σ_s, the fission cross section, Σ_f, and the number of neutrons, ν, emitted for each fission. The (n,2n), (n,3n), ... cross sections are assumed to be zero (but need not be). Thus the total cross section equals the sum of Σ_c, Σ_s, and Σ_f, thereby providing a consistency check on the cross section set. Many references give $(\nu\Sigma_f)$ instead of ν and Σ_f. Since both parameters (not the product) may be required by a code for the problem solution, the product $(\nu\Sigma_f)$ has been split into ν and Σ_f preserving their product and Σ_t. The value of c for k_{eff}=1 in equation 6 is also included in each cross section table. For the reflected spheres, different secondaries ratios, c, are reported with the critical dimension for k_{eff}=1 for various combinations of core and reflector thicknesses. To maintain consistent cross sections with the U-235 set, the parameter, ν, was modified to match c to the literature values.

When anisotropic scattering cross sections are provided, the anisotropic components are designated by Σ_{s_1} and Σ_{s_2}, respectively. Similarly, the isotropic scattering component is designated by Σ_{s_0}.

The value of k_∞, as defined in Appendix A, is given for each cross section set. For finite problems where k_{eff} is unity, the critical dimension, r_c, is listed for each geometry in both mean free paths (to indicate the neutron optical thickness) and in centimeters for the one-dimensional geometries. When available in the literature, the scalar flux values, normalized to the flux at the center

of the fissile material, are also provided. The two-media problems have $c_1 > 1$ for the core region 1 and $c_2 < 1$ for the surrounding reflector region 2. The two-media problems use the cross sections for the nonmultiplying reflector. The critical dimensions for the multiplying medium and reflector thickness are given in both mean free paths and centimeters.

A comparison of the critical dimensions for the different geometries behave as expected; that is, the critical dimension is smallest for the one-dimensional slab and increases for the cylinder and sphere. This behavior is to be expected due to the increased leakage with the curvi-linear geometries. For the reflected geometries, the critical dimension decreases with increasing reflector thickness.

4.1 One-Energy Group Isotropic Scattering

4.1.1 One-Group Pu-239.

One-Energy Group Isotropic Cross Sections

Table 2 gives the one-group, isotropic cross sections for two cases of Pu-239 (c=1.50 and c=1.40) and a H_2O (c=0.90) reflector. The total cross sections are the same for both Pu-239 cases and H_2O as required by the reference for the two-media solutions.

Table 2
One-Group Macroscopic Cross Sections (cm^{-1}) for Pu-239 (c=1.40,1.50) and H_2O (c=0.90)

Material	ν	Σ_f	Σ_c	Σ_s	Σ_t	c
Pu-239 (a)	3.24	0.081600	0.019584	0.225216	0.32640	1.50
Pu-239 (b)	2.84	0.081600	0.019584	0.225216	0.32640	1.40
H_2O (refl)	0.0	0.0	0.032640	0.293760	0.32640	0.90

Infinite Medium (PUa-1-0-IN and PUb-1-0-IN)

Using the cross sections for Pu-239 (a) (problem 1) in Table 2, $k_\infty = 2.612903$ with a constant angular and scalar flux everywhere. Using the cross sections for Pu-239 (b) (problem 5) in Table 2, $k_\infty = 2.290323$ with a constant angular and scalar flux everywhere.

One-Medium Slab, Cylinder, and Sphere Critical Dimensions

The Pu-239 (a) critical dimension, r_c, is listed in Table 3.

Table 3
Critical Dimensions, r_c, for One-Group Bare Pu-239 (c=1.50)

Problem	Identifier	Geometry	r_c (mfp)	r_c (cm)	Reference
2	PUa-1-0-SL	Slab	0.605055	1.853722	[16]

The Pu-239 (b) critical dimensions, r_c, are listed in Table 4. The normalized scalar flux for four spatial positions are given in Table 5 using the same references. The flux ratios for PUb-1-0-CY are only available to four decimal places.

Table 4
Critical Dimensions, r_c, for One-Group Bare Pu-239 (c=1.40)

Problem	Identifier	Geometry	r_c (mfp)	r_c (cm)	Reference
6	PUb-1-0-SL	Slab	0.73660355	2.256751	[35]
7	PUb-1-0-CY	Cylinder	1.396979	4.279960	[36],[37]
8	PUb-1-0-SP	Sphere	1.9853434324	6.082547	[35]

Table 5
Normalized Scalar Fluxes for One-Group Bare Pu-239 (c=1.40)

Problem	Identifier	Geometry	$r/r_c = 0.25$	$r/r_c = 0.5$	$r/r_c = 0.75$	$r/r_c = 1.0$
6	PUb-1-0-SL	Slab	0.9701734	0.8810540	0.7318131	0.4902592
7	PUb-1-0-CY	Cylinder	—	0.8093	—	0.2926
8	PUb-1-0-SP	Sphere	0.93538006	0.75575352	0.49884364	0.19222603

Two-Media Slab and Cylinder Critical Dimensions

The literature values in Tables 6 and 7 give the critical dimensions for Pu-239 (a) for two H_2O reflector thicknesses. The first two-media problem (problem 3) in Table 6 is a special nonsymmetric two-region, Pu-239 and H_2O, problem. The second two-media problem (problem 4) in Table 7 is a symmetric three-region problem with the reflector on both sides of the fissile medium.

Table 6
Critical Dimensions for One-Group Pu-239 Slab (c=1.50) with Non-Symmetric H_2O Reflector (c=0.90)

Problem	Identifier	Geometry	Pu r_c	H_2O thickness	Pu+H_2O Radius	Reference
3	PUa-H2O(1)-1-0-SL	Slab (mfp)	0.482566	1		[16],[55]
		(cm)	1.478450	3.063725	4.542175	

Table 7
Critical Dimensions for One-Group Pu-239 Slab (c=1.50) with H_2O Reflector (c=0.90)

Problem	Identifier	Geometry	Pu r_c	H_2O thickness	Pu+H_2O radius	Reference
4	PUa-H2O(0.5)-1-0-SL	Slab (mfp)	0.43015	0.5		[16],[55]
		(cm)	1.317862	1.531863	2.849725	

The literature values in Table 8 give the critical dimensions for Pu-239 (b) with two H_2O reflector thicknesses.

Table 8
Critical Dimensions for One-Group Pu-239 Cylinder (c=1.40) with H_2O Reflector (c=0.90)

Problem	Identifier	Geometry	Pu r_c	H_2O thickness	Pu+H_2O Radius	Reference
9	PUb-H2O(1)-1-0-CY	Cylinder (mfp)	1.10898	1		[38]
		(cm)	3.397610	3.063725	6.461335	
10	PUb-H2O(10)-1-0-CY	Cylinder (mfp)	1.00452	10		[38]
		(cm)	3.077574	30.637255	33.714829	

4.1.2 One-Group U-235.

One-Group Isotropic Cross Sections

Table 9 gives the one-group, isotropic cross sections for two cases of U-235 and a H_2O reflector. Notice that one-group Σ_t for Pu-239 and U-235 are the same as given in reference [41], but the secondaries ratio, c, differs.

Table 9
One-Group Macroscopic Cross Sections (cm^{-1}) for U-235 (c=1.30)

Material	ν	Σ_f	Σ_c	Σ_s	Σ_t	c
U-235 (a)	2.70	0.065280	0.013056	0.248064	0.32640	1.30
U-235 (b)	2.797101	0.065280	0.013056	0.248064	0.32640	1.3194202
U-235 (c)	2.707308	0.065280	0.013056	0.248064	0.32640	1.3014616
U-235 (d)	2.679198	0.065280	0.013056	0.248064	0.32640	1.2958396
H_2O (refl)	0.0	0.0	0.032640	0.293760	0.32640	0.90

Infinite Medium (Ua-1-0-IN, Ub-1-0-IN, Uc-1-0-IN, and Ud-1-0-IN)

Using the cross sections for U-235 (a) in Table 9, $k_\infty = 2.250000$ (problem 11) with a constant angular and scalar flux everywhere. Using the cross sections for U-235 (b), U-235 (c), and U-235 (d) in Table 9, $k_\infty = 2.330917$ (problem 15), 2.256083 (problem 17), and 2.232667 (problem 19) with a constant angular and scalar flux everywhere, respectively.

One-Medium Slab, Cylinder, and Sphere Critical Dimensions

The critical dimension, r_c, and spatial flux ratios are given in Table 10 and 11 for U-235 (a). The references are the same for both tables.

Table 10
Critical Dimensions, r_c, for One-Group Bare U-235 (c=1.30)

Problem	Identifier	Geometry	r_c (mfp)	r_c (cm)	Reference
12	Ua-1-0-SL	Slab	0.93772556	2.872934	[35]
13	Ua-1-0-CY	Cylinder	1.72500292	5.284935	[36], [37]
14	Ua-1-0-SP	Sphere	2.4248249802	7.428998	[35]

Table 11
Normalized Scalar Fluxes for One-Group Bare U-235 (c=1.30)

Problem	Identifier	Geometry	$r/r_c = 0.25$	$r/r_c = 0.5$	$r/r_c = 0.75$	$r/r_c = 1.0$
12	Ua-1-0-SL	Slab	0.9669506	0.8686259	0.7055218	0.4461912
14	Ua-1-0-SP	Sphere	0.93244907	0.74553332	0.48095413	0.17177706

Two-Media Sphere Critical Dimensions

The literature values in Table 12, give the critical dimensions for U-235 (b), U-235 (c), and U-235 (d) for three spherical H_2O reflector thicknesses.

Table 12
Critical Dimensions for One-Group U-235 Sphere with H_2O Reflector (c=0.90)

Problem	Identifier	Geometry	U r_c	H_2O thickness	U+H_2O Radius	Reference
16	Ub-H2O(1)-1-0-SP	Sphere (mfp)	2	1		[24],[27]
		(cm)	6.12745	3.063725	9.191176	
18	Uc-H2O(2)-1-0-SP	Sphere (mfp)	2	2		[24],[27]
		(cm)	6.12745	6.12745	12.2549	
20	Ud-H2O(3)-1-0-SP	Sphere (mfp)	2	3		[24],[27]
		(cm)	6.12745	9.191176	15.318626	

4.1.3 One-Group U-D_2O Reactor.

One-Group Isotropic Cross Sections

Table 13 gives the one-group, isotropic cross sections for the uranium-D_2O reactor and H_2O reflector. Note that the uranium-D_2O reactor and H_2O reflector have the same total cross section as required by the references for the reflected cylindrical solutions.

Table 13
One-Group Macroscopic Cross Sections (cm^{-1}) for U-D_2O Reactor (c=1.02) and H_2O (c=0.90)

Material	ν	Σ_f	Σ_c	Σ_s	Σ_t	c
U-D_2O	1.70	0.054628	0.027314	0.464338	0.54628	1.02
H_2O (refl)	0.0	0.0	0.054628	0.491652	0.54628	0.90

Infinite Medium (UD2O-1-0-IN)

Using the cross sections for U-D_2O in Table 13, k_∞ = 1.133333 (problem 21) with a constant angular and scalar flux everywhere.

One-Medium Slab, Cylinder, and Sphere Critical Dimensions

The critical dimension, r_c, and spatial flux ratios are listed in Table 14 and 15.

Table 14
Critical Dimensions, r_c, for One-Group Bare U-D_2O Reactor (c=1.02)

Problem	Identifier	Geometry	r_c (mfp)	r_c (cm)	Reference
22	UD2O-1-0-SL	Slab	5.6655054562	10.371065	[35]
23	UD2O-1-0-CY	Cylinder	9.043255	16.554249	[36],[37]
24	UD2O-1-0-SP	Sphere	12.0275320980	22.017156	[35]

Table 15
Normalized Scalar Fluxes for One-Group Bare U-D_2O Reactor (c=1.02)

Problem	Identifier	Geometry	r/r_c = 0.25	r/r_c = 0.5	r/r_c = 0.75	r/r_c = 1.0
22	UD2O-1-0-SL	Slab	0.93945236	0.76504084	0.49690627	0.13893858
24	UD2O-1-0-SP	Sphere	0.91063756	0.67099621	0.35561622	0.04678614

Two-Media Slabs and Cylinders Critical Dimensions

Table 16 gives the U-D_2O critical dimension, r_c, for two H_2O reflector thicknesses.

Table 16
Critical Dimensions for One-Group U-D_2O (c=1.02) Slab and Cylinder with H_2O (c=0.90) Reflector

Problem	Identifier	Geometry	UD_2O r_c	H_2O thickness	UD_2O + H_2O radius	Reference
25	UD2O-H2O(1)-1-0-SL	Slab (mfp)	5.0335	1		[42], [43]
		(cm)	9.214139	1.830563	11.044702	
26	UD2O-H2O(10)-1-0-SL	Slab (mfp)	4.6041	10		[42],[43]
		(cm)	8.428096	18.30563	26.733726	
27	UD2O-H2O(1)-1-0-CY	Cylinder (mfp)	8.411027	1		[38]
		(cm)	15.396916	1.830563	17.227479	
28	UD2O-H2O(10)-1-0-CY	Cylinder (mfp)	7.979325	10		[38]
		(cm)	14.606658	18.30563	32.912288	

4.1.4 One-Group U-235 Reactor.

One-Group Isotropic Cross Sections

Table 17 gives the one-group, isotropic cross sections for the U-235 reactor with a Fe reflector and Na moderator.

Table 17
One-Group Macroscopic Cross Sections (cm^{-1}) for U-235 Reactor, Fe reflector, and Na Moderator

Material	ν	Σ_f	Σ_c	Σ_s	Σ_t	c
U-235 (e)	2.50	0.06922744	0.01013756	0.328042	0.407407	1.230
Fe (refl)	0.0	0.0	0.00046512	0.23209488	0.23256	0.9980
Na (mod)	0.0	0.0	0.0	0.086368032	0.086368032	1.00

Infinite Medium (Uc-1-0-IN)

Using the cross sections for the U-235 reactor in Table 17, k_∞ = 2.1806667 (problem 29) with a constant angular and scalar flux everywhere.

One-Medium Slab Critical Dimensions

Note that this problem is a nonsymmetric four-region problem. The U-235 is surrounded by a Fe cladding on two sides but moderated by Na on one side. The critical dimension, r_c, is listed in Tables 18 and 19.

Table 18
Critical Dimensions, r_c, for One-Group U-235 Reactor

Problem	Identifier	Geometry	Fe thickness	U-235 thickness	Fe thickness	Na thickness	Reference
30	Ue-Fe-Na-1-0-SL	Slab (mfp)	0.0738	2.0858098	0.0738	0.173	[55]
		(cm)	0.317337461	5.119720083	0.317337461	2.002771002	

Table 19
Critical Dimensions, r_c, for One-Group U-235 Reactor

Problem	Identifier	Geometry	Fe thickness	Fe+U	Fe+U+Fe	Fe+U+Fe+Na
30	Ue-Fe-Na-1-0-SL	Slab (cm)	0.317337461	5.437057544	5.754395005	7.757166007

The U-235 (e) critical dimensions, r_c, are listed in Tables 18 and 19. The normalized scalar flux for four spatial positions are given in Table 20 using the same references. These positions correspond to the material boundaries and are normalized by the scalar neutron flux at the left boundary.

Table 20
Normalized Scalar Fluxes for One-Group U-235 Reactor

Problem	Identifier	Geometry	Fe-U	U-Fe	Fe-Na	Na
30	Ue-Fe-Na-1-0-SL	Slab	1.229538	1.49712	1.324899	0.912273

4.2 One-Group Anisotropic Scattering

4.2.1 One-Group Pu-239.

One-Energy Group Anisotropic Cross Sections

Table 21 gives the one-group, anisotropic cross sections for two cases of anisotropic scattering. The first cross section set, Pu-239 (a), includes P_1 and P_2 scattering cross sections, where $\mid \mu \mid < 1/3$. The second cross section set, Pu-239 (b), includes the P_1 and P_2 scattering cross sections where $\mid \mu \mid > 1/3$. **Care must be used to correctly solve this benchmark problem because of the negative scattering for μ near -1.**

Table 21
One-Group Macroscopic Anisotropic Cross Sections (cm^{-1}) for Pu-239 (c=1.40)

Material	ν	Σ_f	Σ_c	Σ_{s0}	Σ_{s1}	Σ_{s2}	Σ_t	c
Pu-239 (a)	2.5	0.266667	0.0	0.733333	0.20	0.075	1.0	1.40
Pu-239 (b)	2.5	0.266667	0.0	0.733333	0.333333	0.125	1.0	1.40

Infinite Medium (PU-1-1-IN)

Using the cross sections for Pu-239 (a) and Pu-239 (b) in Table 21, k_∞ = 2.500000 (problem 31) with a constant angular and scalar flux everywhere. The anisotropic scattering cross sections do not change k_∞.

One-Medium Slab Critical Dimensions

The Pu-239 critical dimensions, r_c, for both P_1 and P_2 problems are listed in Table 22.

Table 22
Critical Dimensions, r_c, for One-Group Bare Pu-239 (c=1.40)

Problem	Identifier	Geometry	r_c (mfp)	r_c (cm)	Reference
32	PUa-1-1-SL	Slab	0.77032	0.77032	[39]
33	PUa-1-2-SL	Slab	0.76378	0.76378	[39]
34	PUb-1-1-SL	Slab	0.79606	0.79606	[39]
35	PUb-1-2-SL	Slab	0.78396	0.78396	[39]

4.2.2 One-Group U-235

One-Energy Group Anisotropic Cross Sections

Table 23 gives the two sets of one-group, anisotropic cross sections for U-235. Notice that the cross sections are the same as in Table 9 with the addition of P_1 scattering cross sections. The first cross section set, U-235 (a), includes P_1 scattering cross sections, where $|\mu| < 1/3$. The second cross section set, U-235 (b), includes the P_1 scattering cross sections where $|\mu| > 1/3$. **Care must be used to correctly solve this benchmark problem because of the negative scattering for μ near -1.**

Table 23
One-Group Macroscopic Anisotropic Cross Sections (cm^{-1}) for U-235 (c=1.30)

Material	ν	Σ_f	Σ_c	Σ_{s_0}	Σ_{s_1}	Σ_t	c
U-235 (a)	2.70	0.065280	0.013056	0.248064	0.042432	0.32640	1.30
U-235 (b)	2.70	0.065280	0.013056	0.248064	0.212160	0.32640	1.30

Infinite Medium (U-1-1-IN)

Using the cross sections for U-235 (a) and U-235 (b) in Table 23, k_∞ = 2.250000 (problem 11) with a constant angular and scalar flux everywhere. The anisotropic scattering cross sections do not change k_∞.

One-Medium Slab Critical Dimensions

The U-235 critical dimensions, r_c, for both P_1 problems are listed in Table 24.

Table 24
Critical Dimensions, r_c, for One-Group Bare U-235 (c=1.30)

Problem	Identifier	Geometry	r_c (mfp)	r_c (cm)	Reference
36	Ua-1-1-CY	Cylinder	1.799866479	5.514296811	[40]
37	Ub-1-1-CY	Cylinder	2.265283130	6.940205668	[40]

4.2.3 One-Group U-D_2O

One-Energy Group Anisotropic Cross Sections

Table 25 gives the two sets of one-group, anisotropic cross sections for U-D_2O reactor. Notice that the cross sections are the same as in Table 13 with the addition of P_1 scattering cross sections. The cross sections set for two U-D_2O cases include P_1 scattering cross sections, where $|\mu| < 1/3$, and a P_1 case where $\mu < 0$ and the scattering cross section is negative. **Care must be used to correctly solve this benchmark problem because of the negative scattering for μ near -1.**

Infinite Medium UD2Oa-1-1-IN, UD2Ob-1-1-IN, and UD2Oc-1-1-IN

Using the cross sections for U-D_2O (a), U-D_2O (b), and U-D_2O (c) in Table 25, k_∞ = 1.205587 (problem 38), 1.227391 (problem 40), and 1.130933 (problem 42), respectively, with a constant angular and scalar flux everywhere. The

Table 25
One-Group Macroscopic Anisotropic Cross Sections (cm^{-1}) for U-D_2O Reactor

Material	ν	Σ_f	Σ_c	Σ_{s_0}	Σ_{s_1}	Σ_t	c
U-D_2O (a)	1.808381	0.054628	0.027314	0.464338	0.056312624	0.54628	1.0308381
U-D_2O (b)	1.841086	0.054628	0.027314	0.464338	0.112982569	0.54628	1.0341086
U-D_2O (c)	1.6964	0.054628	0.027314	0.464338	-0.27850447	0.54628	1.01964

anisotropic scattering cross sections do not change k_∞.

One-Medium Slab Critical Dimensions

The U-D_2O critical dimensions, r_c, for the P_1 problems are listed in Table 26.

Table 26
Critical Dimensions, r_c, for One-Group Bare U-D_2O

Problem	Identifier	Geometry	r_c (mfp)	r_c (cm)	Reference
39	UD2Oa-1-1-SP	Sphere	10	18.30563081	[22]
41	UD2Ob-1-1-SP	Sphere	10	18.30563081	[22]
43	UD2Oc-1-1-SP	Sphere	10	18.30563081	[23]

5 Two-Energy Group Problem Definitions and Results

The isotropic two-energy group cross sections for five bare and two water reflected cases are listed in this section. There are also two linearly anisotropic scattering cross sections sets provided for bare and infinite medium reactors. Unlike the one-group case, there is no flexibility in choosing these values since they are used throughout the literature. The cross sections listed here are similar to Pu-239, [41] U-235,[41] a realistic enriched uranium-aluminum-water assembly [15], a 93% enriched U-235 model of a university research reactor, [15],[44],[45] and a typical large size D_2O reactor with low enrichment of U-235.[15],[44],[45] Also included are critical dimensions for a similar uranium research reactor with a water reflector in an infinite lattice.[43] Again, these problems use cross sections that are reasonable representations of the materials described. These cross sections are **not** general purpose two-group values. The cross sections are used because they are defined in the literature and are intended to be used only to verify algorithm performance and **not** to predict any actual criticality experiments.

The isotropic neutron cross macroscopic sections (cm^{-1}) provided for these problems are the total cross section of group i, Σ_i, the capture (no neutrons emitted) cross section, Σ_{ci}, the within group scattering cross section, Σ_{iis}, the group-to-group scattering cross sections, Σ_{ijs} and Σ_{jis}, the fission cross section, Σ_{if}, the number of neutrons, ν_i, emitted from each fission in a group, and the fission distribution, χ_i.

In this paper, the fast energy group is group 2 to be consistent with most of the references. This notation is the reverse of most nuclear engineering textbooks.

The literature solutions are often based on the group transfer cross sections, Σ_{ij}, given in the references; therefore, the individual cross sections may not be unique. Most references give $(\nu\Sigma_f)_i$ instead of ν_i and Σ_{fi}. Since both parameters (not the product) may be required by a code for the problem solution, the product $(\nu\Sigma_f)_i$ has been split into ν_i and Σ_{fi} preserving their product and Σ_t. The infinite slab lattice problems use a slightly unphysical set of cross sections to possibly stress code verification.

The two sets of linearly anisotropic cross sections provided are extensions of the university research reactor and D_2O cases.[32] The anisotropic scattering component is designated for the in-group and group-to-group scattering cross section by Σ_{iis_1} and Σ_{jis_1}, respectively. Similarly, the isotropic scattering component is designated by Σ_{iis_0} and Σ_{jis_0}.

The value for k_∞ is given for each cross section set. For finite problems, the critical dimension, r_c, is listed in both fast group mean free paths (to indicate the

neutron optical thickness) and in centimeters. For two-media problems, critical dimensions for the inner multiplying medium and outer reflector thickness are given in both fast mean free paths and centimeters. The critical dimensions, r_c, and reflector half thicknesses are also given for a water reflected infinite slab lattice cell. Flux values are given for the university research reactor (a) (problems 54 and 71) at four spatial points. Angular fluxes can be found in the dissertation references.

To distinguish between the different URR fissile material cross section sets, each is labeled with a letter "*a*," "*b*," "*c*," or "*d*", respectively. The infinite slab lattice cell cross sections are similar to the other three cross section sets for the university research reactor and are labeled with URRd identifiers. The literature also uses three different H_2O reflectors. Their cross sections are also labeled with a letter "*a*," "*b*," or "*c*" in the identifier. URR cross section sets "*b*" and "*c*" have thermal upscattering. All other two-group cross sections have no thermal upscattering.

A comparison of the critical dimensions for the different geometries behave as expected; that is, the critical dimension is smallest for the one-dimensional slab and increases for the cylinder and sphere. This behavior is to be expected due to the increased leakage with the curvi-linear geometries. The effect of increased leakage on the critical dimension can be also be seen for the forward peaked linear anisotropically scattering cases. For the reflected geometries, the critical dimension decreases with increasing reflector thickness. However, the critical dimension for the infinite lattice cell *increases* with the increasing moderator thickness. Even though this may seem counter-intuitive, it should be expected because the amount of interaction between the fissile medium and adjacent cells decreases with increasing moderator half thickness.[43]

5.1 Isotropic Scattering

5.1.1 Two-Group Pu-239.

Two-Group Isotropic Cross Sections

Tables 27 and 28 give the two-group, isotropic cross sections for Pu-239.

Table 27
Fast Energy Group Macroscopic Cross Sections (cm^{-1}) for Pu-239

Material	ν_2	Σ_{2f}	Σ_{2c}	Σ_{22s}	Σ_{12s}	Σ_2	χ_2
Pu-239	3.10	0.0936	0.00480	0.0792	0.0432	0.2208	0.575

Table 28
Slow Energy Group Macroscopic Cross Sections (cm^{-1}) for Pu-239

Material	ν_1	Σ_{1f}	Σ_{1c}	Σ_{11s}	Σ_{21s}	Σ_1	χ_1
Pu-239	2.93	0.08544	0.0144	0.23616	0.0	0.3360	0.425

Infinite Medium (PU-2-0-IN)

Using the two-group isotropic Pu-239 cross section set from Tables 27 and 28, k_∞ = 2.683767 (problem 44) with a constant group angular and scalar flux and a group 2 to group 1 flux ratio = 0.675229.

One-Medium Slab and Sphere Critical Dimensions

The critical dimensions, r_c, are listed in Table 29.

Table 29
Critical Dimensions, r_c, for Two-Group Bare Pu-239

Problem	Identifier	Geometry	r_c (mfp)	r_c (cm)	Reference
45	PU-2-0-SL	Slab	0.396469	1.795602	[15], [44], [45]
46	PU-2-0-SP	Sphere	1.15513	5.231567	[15], [44], [45]

5.1.2 Two-Group U-235.

Two-Group Cross Sections

Tables 30 and 31 give the two-group, isotropic cross sections for U-235.

Table 30
Fast Energy Group Macroscopic Cross Sections (cm^{-1}) for U-235

Material	ν_2	Σ_{2f}	Σ_{2c}	Σ_{22s}	Σ_{12s}	Σ_2	χ_2
U-235	2.70	0.06192	0.00384	0.078240	0.0720	0.2160	0.575

Table 31
Slow Energy Group Macroscopic Cross Sections (cm^{-1}) for U-235

Material	ν_1	Σ_{1f}	Σ_{1c}	Σ_{11s}	Σ_{21s}	Σ_1	χ_1
U-235	2.50	0.06912	0.01344	0.26304	0.0	0.3456	0.425

Infinite Medium (U-2-0-IN)

Using the two-group U-235 cross section set from Tables 30 and 31, $k_\infty = 2.216349$ (problem 47) with a constant group angular and scalar flux and the group 2 to group 1 flux ratio = 0.474967.

One-Medium Slab and Sphere Critical Dimensions

The critical dimensions, r_c, are listed in Table 32.

Table 32
Critical Dimension, r_c, for Two-Group Bare U-235

Problem	Identifier	Geometry	r_c (mfp)	r_c (cm)	Reference
48	U-2-0-SL	Slab	0.649377	3.006375	[15], [44], [45]
49	U-2-0-SP	Sphere	1.70844	7.909444	[15]

5.1.3 Two-Group Uranium-Aluminum-Water Assembly.

Two-Group Isotropic Cross Sections

Tables 33 and 34 gives the two-group, isotropic cross sections for the uranium, aluminum, and water assembly.

Table 33
Fast Energy Group Macroscopic Cross Sections(cm^{-1}) for U-Al

Material	ν_2	Σ_{2f}	Σ_{2c}	Σ_{22s}	Σ_{12s}	Σ_2	χ_2
U-Al	0.0	0.0	0.000217	0.247516	0.020432	0.268165	1.0

Table 34
Slow Energy Group Macroscopic Cross Sections (cm^{-1}) for U-Al

Material	ν_1	Σ_{1f}	Σ_{1c}	Σ_{11s}	Σ_{21s}	Σ_1	χ_1
U-Al	2.830023	0.060706	0.003143	1.213127	0.0	1.276976	0.0

Infinite Medium (UAL-2-0-IN)

With the two-group cross section set from Tables 33 and 34, $k_\infty = 2.662437$ (problem 50) and the group 2 to group 1 flux ratio = 3.124951.

One-Medium Slab and Sphere Critical Dimensions

Using the cross sections given in Tables 33 and 34, the critical dimensions, r_c, are given in Table 35.

Table 35
Critical Dimensions, r_c, for Two-Group Uranium-Aluminum-Water Assembly

Problem	Identifier	Geometry	r_c (mfp)	r_c (cm)	Reference
51	UAL-2-0-SL	Slab	2.09994	7.830776	[15], [44], [45]
52	UAL-2-0-SP	Sphere	4.73786	17.66770	[15]

5.1.4 Two-Group Uranium Research Reactor.

Two-Group Isotropic Cross Sections

The cross sections for the one-medium (a), two-media (b and c), and infinite slab lattice (d) cases are different and are therefore listed separately. Tables 36 and 37 gives the two-group, one-medium, isotropic cross sections for the 93% enriched uranium bare university research reactor.

Table 36
Fast Energy Group Macroscopic Cross Sections (cm^{-1}) for Research Reactor (a)

Material	ν_2	Σ_{2f}	Σ_{2c}	Σ_{22s}	Σ_{12s}	Σ_2	χ_2
Research Reactor (a)	2.50	0.0010484	0.0010046	0.62568	0.029227	0.65696	1.0

Table 37
Slow Energy Group Macroscopic Cross Sections (cm^{-1}) for Research Reactor (a)

Material	ν_1	Σ_{1f}	Σ_{1c}	Σ_{11s}	Σ_{21s}	Σ_1	χ_1
Research Reactor (a)	2.50	0.050632	0.025788	2.44383	0.0	2.52025	0.0

Infinite Medium (URRa-2-0-IN)

The test set uses the two-group enriched U-235 cross section set for the research reactor in Tables 36 and 37 with $k_\infty = 1.631452$ (problem 53) and the group 2 to group 1 flux ratio = 2.614706.

One-Medium Slab and Sphere Critical Dimensions

The critical dimensions, r_c, are listed in Table 38.

Table 38
Critical Dimensions, r_c, for Two-Group Bare Research Reactor (a)

Problem	Identifier	Geometry	r_c (mfp)	r_c (cm)	Reference
54	URRa-2-0-SL	Slab	4.97112	7.566853	[15],[44], [45]
55	URRa-2-0-SP	Sphere	10.5441	16.049836	[15]

One-Medium Slab Scalar Neutron Fluxes

Table 39 gives the normalized scalar neutron flux for the two-group bare research reactor (a) at four spatial points [45]. All values are normalized with the fast group flux at the center.

Table 39
Normalized Scalar Fluxes for Two-Group Bare Research Reactor (a)

Problem	Identifier	Geometry	Energy Group	$r/r_c = 0.241394$	$r/r_c = 0.502905$	$r/r_c = 0.744300$	$r/r_c = 1.0$
54	URRa-2-0-SL	Slab	Fast	0.943363	0.761973	0.504012	0.147598
			Slow	0.340124	0.273056	0.173845	0.0212324

Two-Media Cross Sections for Slab Geometry

The cross sections for the two-media problems for the uranium research reactor are given for two different multiplying media with one nonmultiplying reflector. The two multiplying materials are labeled (*b*) and (*c*), respectively. The multiplying region consists of an H_2O + U-235 mixture surrounded by an H_2O reflector. The results in the literature for case (*c*) only include the infinite water reflector. The cross sections are given in Tables 40 and 41. Notice that this problem allows thermal upscattering in both multiplying and nonmultiplying regions.

Table 40
Fast Energy Group Macroscopic Cross Sections (cm^{-1}) for Research Reactor (b), (c) and H_2O Reflector (a)

Material	ν_2	Σ_{2f}	Σ_{2c}	Σ_{22s}	Σ_{12s}	Σ_2	χ_2
Research Reactor (b)	2.50	0.000836	0.001104	0.83892	0.04635	0.88721	1.0
Research Reactor (c)	2.50	0.001648	0.001472	0.83807	0.04536	0.88655	1.0
H_2O (a) (refl)	0.0	0.0	0.00074	0.83975	0.04749	0.88798	0.0

Table 41
Slow Energy Group Macroscopic Cross Sections (cm^{-1}) for Research Reactor (b), (c) and H_2O Reflector (a)

Material	ν_1	Σ_{1f}	Σ_{1c}	Σ_{11s}	Σ_{21s}	Σ_1	χ_1
Research Reactor (b)	2.50	0.029564	0.024069	2.9183	0.000767	2.9727	0.0
Research Reactor (c)	2.50	0.057296	0.029244	2.8751	0.00116	2.9628	0.0
H_2O (a) (refl)	0.0	0.0	0.018564	2.9676	0.000336	2.9865	0.0

Infinite Medium (URRb-2-0-IN and URRc-2-0-IN)

Using the two-group cross section set for the research reactor (*b*) from Tables 40 and 41, $k_\infty = 1.365821$ (problem 56) with a constant group angular and scalar flux and the group 2 to group 1 flux ratio = 1.173679. Using the two-group cross section set for research reactor (*c*) from Tables 40 and 41, $k_\infty = 1.633380$ (problem 57)

with a constant group angular and scalar flux and the group 2 to group 1 flux ratio = 1.933422.

Two-Media Slab Critical Dimensions

Using the cross sections in Tables 40 and 41 for the H_2O + U-235 research reactor and the H_2O reflector, the critical dimensions are given in Table 42. The mfp results use the group 2 total macroscopic cross section of region i to obtain the dimensions in cm.

Table 42
Critical Dimensions for Two-Group Research Reactor (b),(c) with H_2O Reflector (a)

Problem	Identifier	Geometry	U-235, r_c	H_2O Width	U-235 + H_2O Width	Ref.
58	URRb-II2Oa(1)-2-0-SL	Slab (mfp)	5.94147	1		[46]
		(cm)	6.696802	1.126152	7.822954	
59	URRb-H2Oa(5)-2-0-SL	Slab (mfp)	4.31485	5		[46]
		(cm)	4.863392	5.630757	10.494149	
60	URRb-H2Oa(IN)-2-0-SL	Slab (mfp)	4.15767	∞	∞	[46]
		(cm)	4.686230	∞	∞	
61	URRc-H2Oa(IN)-2-0-SL	Slab (mfp)	2.1826	∞	∞	[46]
		(cm)	2.461903	∞	∞	

Two-Media Cross Sections for Infinite Slab Lattice Cell

The two-media cross sections are given in Tables 43 and 44 for a similar uranium enriched university research reactor. The ν_2 is slightly unphysical to stress criticality codes. Two different reflector materials are also given in Tables 43 and 44. The problems that use these cross sections are for an infinite slab lattice cell.

Table 43
Fast Group Macroscopic Cross Sections (cm^{-1}) for Research Reactor(d) and H_2O Reflector (b), (c)

Material	ν_2	Σ_{2f}	Σ_{2c}	Σ_{22s}	Σ_{12s}	Σ_2	χ_2
Research Reactor (d)	1.004	0.61475	0.0019662	0.0	0.0342008	0.650917	1.0
H_2O (b) (refl)	0.0	0.0	8.480293×10^{-6}	0.1096742149	0.001000595707	0.1106832906	0.0
H_2O (c) (refl)	0.0	0.0	4.97229×10^{-4}	1.226381244	0.1046395340	1.331518007	0.0

Table 44
Slow Group Macroscopic Cross Sections (cm^{-1}) for Research Reactor(d) and H_2O Reflector (b), (c)

Material	ν_1	Σ_{1f}	Σ_{1c}	Σ_{11s}	Σ_{21s}	Σ_1	χ_1
Research Reactor (d)	2.50	0.045704	0.023496	2.06880	0.0	2.13800	0.0
H_2O (b) (refl)	0.0	0.0	0.00016	0.36339	0.0	0.36355	0.0
H_2O (c) (refl)	0.0	0.0	0.0188	4.35470	0.0	4.37350	0.0

Infinite Medium (URRd-2-0-IN)

The test set uses the two-group cross section set for the research reactor in Tables 43 and 44 with $k_\infty = 1.034970$ (problem 62) and the group 2 to group 1 flux ratio = 2.023344.

Two-Media Infinite Slab Lattice Cell Critical Dimensions

Using the cross sections in Tables 43 and 44 for the enriched uranium research reactor with a H_2O reflector, the critical dimensions for an infinite slab lattice cell as shown in Figure 2 are given in Table 45. Because this is an infinite slab lattice cell with reflecting outer boundaries, notice that the moderator half thickness is given.

Table 45
Critical Dimensions for Two-Group Infinite Slab Lattice Cell and H_2O Reflector (b), (c)

Problem	Identifier	Geometry	U-235, r_c	H_2O Width	U-235+H_2O Width	Ref.
63	URRd-H2Ob(1)-2-0-ISLC	Inf. Slab (mfp)	0.02142	1		[43]
		Lat. Cell (cm)	0.0329074	9.034787	9.067695	
64	URRd-H2Ob(10)-2-0-ISLC	Inf. Slab (mfp)	0.29951	10		[43]
		Lat. Cell (cm)	0.460135	90.347875	90.808010	
65	URRd-H2Oc(1)-2-0-ISLC	Inf. Slab (mfp)	0.22197	1		[43]
		Lat. Cell (cm)	0.341011	0.751023	1.092034	
66	URRd-H2Oc(10)-2-0-ISLC	Inf. Slab (mfp)	1.7699	10		[43]
		Lat. Cell (cm)	2.719087	7.510225	10.229312	

5.1.5 Two-Group U-D_2O Reactor.

Two-Group Isotropic Cross Sections

Tables 46 and 47 give the two-group, isotropic cross sections for the uranium-D_2O system.

Table 46
Fast Energy Group Macroscopic Cross Sections (cm^{-1}) for U-D_2O

Material	ν_2	Σ_{2f}	Σ_{2c}	Σ_{22s}	Σ_{12s}	Σ_2	χ_2
U-D_2O	2.50	0.002817	0.0087078	0.31980	0.0045552	0.33588	1.0

Table 47
Slow Energy Group Macroscopic Cross Sections (cm^{-1}) for U-D_2O

Material	ν_1	Σ_{1f}	Σ_{1c}	Σ_{11s}	Σ_{21s}	Σ_1	χ_1
U-D_2O	2.50	0.097	0.02518	0.42410	0.0	0.54628	0.0

Infinite Medium (UD2O-2-0-IN)

The test set uses the two-group U-D_2O cross section set from Tables 46 and 47 with $k_\infty = 1.000221$ (problem 67) and the group 2 to group 1 flux ratio = 26.822093.

One-Medium Slab and Sphere Critical Dimensions

The critical dimensions, r_c, are listed in Table 48.

Table 48
Critical Dimension, r_c, for Two-Group D_2O System

Problem	Identifier	Geometry	r_c (mfp)	r_c (cm)	Reference
68	UD2O-2-0-SL	Slab	284.367	846.632726	[15], [44], [45]
69	UD2O-2-0-SP	Sphere	569.430	1695.337621	[15]

5.2 Linearly Anisotropic Scattering

The anisotropic scattering cross sections for the enriched U-235 research reactor and U-D_2O reactor cases are the same as the isotropic set with the addition of the anisotropic cross sections, Σ_{22s_1}, Σ_{12s_1}, and Σ_{11s_1}.

5.2.1 Two-Group Uranium Research Reactor.

Two-Group Anisotropic Macroscopic Cross Sections

Tables 49 and 50 gives the two-group, linearly anisotropic cross sections for the research reactor. **Care must be used to correctly solve this benchmark problem because of the negative scattering for μ near -1.**

Table 49
Fast Group Cross Sections for Linearly Anisotropic Scattering (cm^{-1}) Research Reactor (a)

Material	ν_2	Σ_{2f}	Σ_{2c}	Σ_{22s_0}	Σ_{22s_1}	Σ_{12s_0}	Σ_{12s_1}	Σ_2	χ_2
Research Reactor (a)	2.50	0.0010484	0.0010046	0.62568	0.27459	0.029227	0.0075737	0.65696	1.0

Table 50
Slow Group Cross Sections for Linearly Anisotropic Scattering (cm^{-1}) Research Reactor (a)

Material	ν_1	Σ_{1f}	Σ_{1c}	Σ_{11s_0}	Σ_{11s_1}	Σ_{21s}	Σ_1	χ_1
Research Reactor (a)	2.50	0.050632	0.025788	2.44383	0.83318	0.0	2.52025	0.0

Infinite Medium (URRa-2-1-IN)

The test set uses the two-group enriched U-235 cross section set from Tables 49 and 50 with k_∞ = 1.631452 (problem 70) and the group 2 to group 1 flux ratio = 2.614706.

One-Medium Slab Critical Dimension

The critical dimensions are listed in Table 51.

Table 51
Critical Dimension, r_c, for Two-Group Linearly Anisotropic Scattering Research Reactor (a)

Problem	Identifier	Geometry	r_c (mfp)	r_c (cm)	Reference
71	URRa-2-1-SL	Slab	6.2384	9.4959	[34]

One-Medium Slab Scalar Neutron Fluxes

Table 52 gives the normalized scalar neutron flux for the two-group bare research reactor (a) with linearly anisotropic scattering at four spatial points.[32] All values are normalized with the fast group flux at the center.

Table 52
Normalized Scalar Fluxes for Two-Group Bare Research Reactor (a)

Problem	Identifier	Geometry	Energy Group	$r/r_c = 0.20$	$r/r_c = 0.50$	$r/r_c = 0.80$	$r/r_c = 1.0$
71	URRa-2-1-SL	Slab	Fast	0.963873	0.781389	0.472787	0.189578
			Slow	0.349006	0.280870	0.157376	0.0277639

5.2.2 Two-Group U-D_2O Reactor.

Two-Group Anisotropic Macroscopic Cross Sections

Tables 53 and 54 gives the two-group, linearly anisotropic cross sections for the U-D_2O system.

Table 53
Fast Energy Group Cross Sections for Linearly Anisotropic Scattering (cm^{-1}) for U-D_2O

Material	ν_2	Σ_{2f}	Σ_{2c}	Σ_{22s_0}	Σ_{22s_1}	Σ_{12s_0}	Σ_{12s_1}	Σ_2	χ_2
D_2O	2.50	0.0028172	0.0087078	0.31980	0.06694	0.004555	-0.0003972	0.33588	1.0

Table 54
Slow Energy Group Cross Sections for Linearly Anisotropic Scattering (cm^{-1}) for U-D_2O

Material	ν_1	Σ_{1f}	Σ_{1c}	Σ_{11s_0}	Σ_{11s_1}	Σ_{21s}	Σ_1	χ_1
D_2O	2.50	0.097	0.02518	0.42410	0.05439	0.0	0.54628	0.0

Infinite Medium (UD2O-2-1-IN)

The test set uses the two-group linearly anisotropic D_2O cross section set from Tables 53 and 54 with $k_\infty = 1.000227$ (problem 72) and the group 2 to group 1 flux

ratio = 26.823271.

One-Medium Slab Critical Dimension

The critical dimension, r_c, is listed in Table 55.

Table 55
Critical Dimension, r_c, for Two-Group Linearly Anisotropic Scattering for U-D_2O Reactor

Problem	Identifier	Geometry	r_c (mfp)	r_c (cm)	Reference
73	UD2O-2-1-SL	Slab	312.18	929.45	[34]

6 Three-Energy Group Problem Definitions and Results

A three-energy group isotropic infinite medium problem is defined in this section. The derivation appears in Appendix A.[47],[53] This problem assumes no thermal upscattering and no fission neutrons born in the slowest energy group.

The fast energy group is group 3 to be consistent with most of the references. Again, this notation is the reverse of most nuclear engineering textbooks.

The cross sections listed here are similar to the uranium university research reactors. Again, this problem uses cross sections that are reasonable representations of the materials described and are **not** general purpose values. The cross sections are intended to be used to verify algorithm performance and **not** to predict criticality experiments. The cross sections are from [47] and are derived in Appendix A.

Infinite Medium (URR-3-0-IN)

Using the three-group cross section set from Tables 56, 57, and 58, k_∞ = 1.600000 (problem 74) with a constant group angular and scalar flux and the group 2 to group 3 flux ratio = 0.480, the group 1 to group 2 flux ratio = 0.3125, and the group 1 to group 3 flux ratio = 0.150.

Table 56
Fast Energy Group Macroscopic Cross Sections (cm^{-1}) for Research Reactor

Material	ν_3	Σ_{3f}	Σ_{3c}	Σ_{33s}	Σ_{23s}	Σ_{13s}	Σ_3	χ_3
Research Reactor	3.0	0.006	0.006	0.024	0.171	0.033	0.240	0.96

Table 57
Middle Energy Group Macroscopic Cross Sections (cm^{-1}) for Research Reactor

Material	ν_2	Σ_{2f}	Σ_{2c}	Σ_{22s}	Σ_{32s}	Σ_{12s}	Σ_2	χ_2
Research Reactor	2.50	0.060	0.040	0.60	0.0	0.275	0.975	0.04

Table 58
Slow Energy Group Macroscopic Cross Sections (cm^{-1}) for Research Reactor

Material	ν_1	Σ_{1f}	Σ_{1c}	Σ_{11s}	Σ_{21s}	Σ_{31s}	Σ_1	χ_1
Research Reactor	2.0	0.90	0.20	2.0	0.0	0.0	3.10	0.0

7 Six-Energy Group Problem Definitions and Results

A six-energy group isotropic infinite medium problem comprised of two coupled three-energy group cross sections used in URR-3-0-IN is defined in this section. This test problem defines a six group cross section set [48] such that energy groups 6 and 1, 5 and 2, and 4 and 3 are equivalent. The top three groups are decoupled from the lower three groups except for the fission distribution, χ_i, which affects energy groups 6, 5, 2, and 1. Energy group 6 (group 1) scatters to groups 5 and 4 (groups 2 and 3). Energy group 5 (group 2) scatters to group 4 (group 3). Energy group 4 (group 3) self-scatters only. Since groups 1,2, and 3 are upscatter equivalents of groups 6, 5, and 4, respectively, this problem should only be used with codes that allow for thermal upscattering.

Infinite Medium (URR-6-0-IN)

Since this problem is comprised of problem URR-3-0-IN cross sections with modified χ_i values, the final k_∞ value and flux ratios will not change. Using the six-group cross section set from Tables 59, 60, 61 62, 63, and 64, k_∞ = 1.600000 (problem 75) with a constant angular and scalar flux in each group. The group 5 to group 6 and group 2 to group 1 flux ratio = 0.480, the group 4 to group 5 and group 3 to group 2 flux ratio = 0.3125, and a group 4 to group 6 and group 3 to group 1 flux ratio = 0.150. These ratios are the same as in the three-group problem.

Table 59
Fast Energy Group 6 Macroscopic Cross Sections (cm^{-1}) for Research Reactor

Material	ν_6	Σ_{6f}	Σ_{6c}	Σ_{66s}	Σ_{56s}	Σ_{46s}	Σ_6	χ_6
Research Reactor	3.0	0.006	0.006	0.024	0.171	0.033	0.240	0.48

Table 60
Energy Group 5 Macroscopic Cross Sections (cm^{-1}) for Research Reactor

Material	ν_5	Σ_{5f}	Σ_{5c}	Σ_{55s}	Σ_{65s}	Σ_{45s}	Σ_5	χ_5
Research Reactor	2.50	0.060	0.040	0.60	0.0	0.275	0.975	0.02

Table 61
Energy Group 4 Macroscopic Cross Sections (cm^{-1}) for Research Reactor

Material	ν_4	Σ_{4f}	Σ_{4c}	Σ_{44s}	Σ_{54s}	Σ_{64s}	Σ_4	χ_4
Research Reactor	2.0	0.90	0.20	2.0	0.0	0.0	3.10	0.0

Table 62
Energy Group 3 Macroscopic Cross Sections (cm^{-1}) for Research Reactor

Material	ν_3	Σ_{3f}	Σ_{3c}	Σ_{33s}	Σ_{23s}	Σ_{13s}	Σ_3	χ_3
Research Reactor	2.0	0.90	0.20	2.0	0.0	0.0	3.10	0.0

Table 63
Energy Group 2 Macroscopic Cross Sections (cm^{-1}) for Research Reactor

Material	ν_2	Σ_{2f}	Σ_{2c}	Σ_{22s}	Σ_{12s}	Σ_{32s}	Σ_2	χ_2
Research Reactor	2.50	0.060	0.040	0.60	0.0	0.275	0.975	0.02

Table 64
Slow Energy Group 1 Macroscopic Cross Sections (cm^{-1}) for Research Reactor

Material	ν_1	Σ_{1f}	Σ_{1c}	Σ_{11s}	Σ_{21s}	Σ_{31s}	Σ_1	χ_1
Research Reactor	3.0	0.006	0.006	0.024	0.171	0.033	0.240	0.48

8 Summary

In this paper, we have documented 75 problem descriptions with precise results for the critical dimensions, k_{eff} eigenvalue, and some eigenfunction (scalar neutron flux) results for infinite, slab, cylindrical, and spherical geometries for one- and two-energy group, multiple-media, and both isotropic and linearly anisotropic scattering using the listed references. We have not given a complete listing of every referenced result that has been published. Instead, we have included the references that provide both true transport solutions and enough information to reproduce the results. Several other references are included for reference completeness. All test set problems specifications and results are from peer reviewed journals, and have, in many cases, been solved numerically by more than one analytic method. These calculated values for k_{eff} and the scalar neutron flux are believed to be accurate to at least five decimal places. Criticality codes can be verified using these analytic benchmark test problems.

9 ACKNOWLEDGMENTS

The authors would like to thank the following people for their role in making this document as correct and useful as possible: R.E. Alcouffe, R.A. Axford (U of Illinois), G.E. Bosler, F.B. Brown, J.D. Court, B.D. Ganapol (U of Arizona), R.P. Gardner (NCSU), D.E. Kornreich, E.W. Larsen (U of Michigan), R.C. Little, R.D. O'Dell, L.M. Petrie (ORNL), A.K. Prinja (UNM), J.E. Stewart, and P.P. Whalen. R.D. O'Dell provided the three- and six-group infinite medium problems.

References

[1] Briesmeister, J.F. "MCNP - A General Purpose Monte Carlo N-Particle Transport Code," Version 4B LA-12625-M.

[2] Alcouffe, R.E., Baker, R.S., Brinkley, F.W., Marr, D.R., O'Dell, R.D. and Walters, W.F. "DANTSYS: A Diffusion Accelerated Neutràl Particle Transport Code System," LA-12969-M, Los Alamos National Laboratory (1995).

[3] Parsons, D.K., Sood, A., Forster, R.A., and Little, R.C. "An Analytic Benchmark Test Set for Criticality Code Verificaiton and Its Application to MCNP and DANTSYS" International Conference on Mathematics and Computation, Reactor Physics and Environmental Analysis, Madrid, Spain (1999).

[4] Parsons, D.K., Sood, A., Forster, R.A., and Little, R.C."Verification of MCNP and DANTSYS with the Analytic Benchmark Test Set" Sixth International Conference on Nuclear Criticality Safety, Versailles, France (1999).

[5] Sood, A., Forster, R.A., and Parsons, D.K."Analytical Benchmark Test Set for Criticality Code Verification" Sixth International Conference on Nuclear Criticality Safety, Versailles, France (1999).

[6] Sood, A., Forster, R.A., and Parsons, D.K."Analytical Benchmark Test Set for Criticality Code Verification" LA-13511 (1999).

[7] "IEEE Software Engineering Standards Collection - Spring 1991 Edition" *IEEE, Inc* (1991).

[8] Zoldi, C.A. "A Numerical and Experimental Study of a Shock-Accelerated Heavy Gas Cylinder" *PhD. Thesis, State University of New York, Stony Brook* (2002).

[9] Argonne National Laboratory "Argonne Code Center: Benchmark Problem Book" *Mathematics and Computation Division of the American Nuclear Society*, ANL-7416 (1968).

[10] Briggs, J.B. Criticality Safety Benchmark Specification Handbook *NEA/NSC/DOC (95)03 I Volume I.*

[11] Petrie, L.M. LA-12556-C, Proceedings of the First Annual Nuclear Criticality Safety Technology Project. **18** (1992).

[12] Lee, C.E. and Carruthers, L.M. "Comparison of S_N Quadrature Methods in Benchmark Criticality Calculations" *LA-9751-MS UC-82* (1983).

[13] Case, K.M. and Zweifel, P.F. "Linear Transport Theory," *Addison-Wesley Publ. Co.* , Reading, Mass. (1967).

[14] Grandjean, P. and Siewert, C.E. "The F_N Method in Neutron Transport Theory. Part II: Applications and Numerical Results" *Nucl. Sci. Eng.*, **69**, 161 (1979).

[15] Siewert, C.E. and Thomas, J.R. "On Two-Group Critical Problems in Neutron Transport Theory" *Nucl. Sci. Eng.* **94**, 264 (1986).

[16] Kornreich, D.E., and Ganapol, B.D. "The Green's Function Method For Nuclear Engineering Applications" *Nucl. Sci. Eng.*, **126**, 293 (1997).

[17] Shuttleworth, T. "The Verification of Monte Carlo Codes in Middle Earth" *Proceedings of 8th International Conference on Radiation Shielding*, p 1148 (1994).

[18] Gelbard, E.M. and Prael, R.E. "Computation of Standard Deviations in Eigenvalue Calculations" *Prog. Nucl. Energy*, **24**, 237 (1990).

[19] Duderstadt, J.J, and Hamilton, L.J. "Nuclear Reactor Analysis, " *John Wiley and Sons*, NY (1976).

[20] Atalay, M.A. "The Reflected Slab and Sphere Criticality Problem with Anisotropic Scattering in One-Speed Neutron Transport Theory" *Prog. Nucl. Energy*, **31**, 299 (1997).

[21] Atalay, M.A. "The Critical Slab Problem for Reflecting Boundary Conditions in One-Speed Neutron Transport Theory" *Ann. Nucl. Energy*, **23**, 183 (1996).

[22] Dahl, E.B. and Sjostrand, N.G. "Eigenvalue Spectrum of Multiplying Slabs and Spheres for Monoenergetic Neutrons with Anisotropic Scattering" *Nucl. Sci. Eng.*, **69**, 114 (1979).

[23] Sahni, D.C. Dahl, E.B., and Sjostrand, N.G. "Real Criticality Eigenvalues of One-Speed Linear Transport Operator" *Trans. Th. Stat. Phy*, **24**, 1295 (1995).

[24] Garis, N.S. "One-Speed Neutron Transport Eigenvalues for Reflected Slabs and Spheres" *Nucl. Sci. Eng.*, **107**, 343 (1991).

[25] Sahni, D.C. and Sjostrand, N.G. "Critical and Time Eigenvalues in One-Speed Neutron Transport" *Prog. Nucl. Energy*, **23**, 3, 241 (1990).

[26] Sahni, D.C. "Some New Results Pertaining to Criticality and Time Eigenvalues of One-Speed Neutron Transport Equation" *Prog. Nucl. Energy*, **30**, 3, 305 (1996).

[27] Sjostrand, N.G. "Criticality of Reflected Spherical Reactors For Neutrons of One-Speed" *Prog. Nucl. Energy*, **13**, 533 (1986).

[28] Bell, G.I. and Glasstone, S. "Nuclear Reactor Theory," *Van Nostrand Reinhold Co.* (1970).

[29] Burkart, A.R., Ishiguro, Y., and Siewert, C.E. "Neutron Transport in Two Dissimilar Media with Anisotropic Scattering," *Nucl. Sci. Eng.*, **61**, 72 (1976).

[30] Burkart, A. R. "The Application of Invariance Principles to Critical Problems in Reflected Reactors" *PhD. Thesis North Carolina State University* (1975).

[31] Boffi, V.C., Molinari, V.G. and Spiga, G. "Anisotropy of Scattering and Fission in Neutron Transport Theory," *Nucl. Sci. Eng.*, **64**, 823 (1977).

[32] Bosler, G.E. "Critical Slab Solution to the Two-Group Neutron Transport Equation for Linearly Anisotropic Scattering" *PhD. Thesis University of Virginia* (1972).

[33] Bosler, G.E. and Metcalf, D.R. "Critical Slab Solution to the Two-Group Neutron Transport Equation for Linearly Anisotropic Scattering" *Trans. Am. Nucl. Soc* **15**, 913 (1972).

[34] Ishiguro, Y. "Two-Group Neutron-Transport Theory with Linearly Anisotropic Scattering: Half-Range Orthogonality and Critical Slab Problem" *Instituto de Energia Atomica*, **306** Sao Paulo, Brazil (1973).

[35] Kaper, H.G., Lindeman, A.J., and Leaf, G.K. "Benchmark Values for the Slab and Sphere Criticality Problem in One-Group Neutron Transport Theory" *Nucl. Sci. Eng.*, **54**, 94 (1974).

[36] Westfall, R.M. "Benchmark Solutions for the Infinite Critical Cylinder" *Trans. Am. Nucl. Soc.*, **44**, 281 (1983).

[37] Westfall, R.M. and Metcalf, D.R. "Exact Solution of the Transport Equation for Critical Cylindrical Configurations" *Trans. Am. Nucl. Soc.*, **15**, 266 (1972).

[38] Westfall, R.M. and Metcalf, D.R. "Singular Eigenfunction Solution of the Monoenergetic Neutron Transport Equation for Finite Radially Reflected Critical Cylinders" *Nucl. Sci. Eng.*, **52**, 1 (1973).

[39] Lathrop, K.D. and Leonard, A. "Comparisons of Exact and S_N Solutions of the Monoenergetic Critical Equation with Anisotropic Scattering" *Nucl. Sci. Eng.*, **22**, 115 (1965).

[40] Sanchez, R. and Ganapol, B.D. "Benchmark Values for Monoenergetic Neutron Transport in One-Dimensional Cylindrical Geometry with Linearly Anisotropic Scattering" *Nucl. Sci. Eng.*, **64**, 61 (1983).

[41] Argonne National Laboratory "Reactor Physics Constants" *United States Atomic Energy Commission*, ANL-5800 (1963).

[42] Stewart, J.E. and Metcalf, D.R. "Monoenergetic Neutron Transport in a Finite Critical Reflected Slab System" *Trans. Am. Nucl. Soc.*, **15**, 267 (1972).

[43] Stewart, J.E. "Two-Media Solutions to the Neutron Transport Equation" *PhD. Thesis University of Virginia* (1974).

[44] Forster, R.A. and Metcalf, D.R. "Two-Group Transport Solutions to the One-Dimensional Critical Slab Problem" *Trans. Am. Nucl. Soc.*, **12**, 637 (1969).

[45] Forster, R.A. "Two-Group Critical Slab Problem" *PhD. Thesis University of Virginia*, (1970).

[46] Ishiguro,Y. and Garcia, R.D.M. "Two-Media Problems in Two-Group Neutron Transport Theory" *Nucl. Sci. Eng.*, **68**, 99 (1978).

[47] O'Dell, R.D. "QA Problem-3 Group k_∞ Calculation" Private Communication (1998).

[48] O'Dell, R.D. "QA Test 2: Upscatter Convergence" Private Communication (1998).

[49] Henry, A.F. "Nuclear-Reactor Analysis" *MIT Press*, Cambridge, MA, (1975).

[50] Lewis, E.E. and Miller, W.F. "Computational Methods in Neutron Transport," *American Nuclear Society, Inc*, La Grange Park, Il (1993).

[51] Whalen, P.P. Private Communication (1998).

[52] Parsons, D.K. and Nigg, D.W. "Extension of the Analytic Nodal Method for Four Energy Groups" **INEL EGG-PBS-6821** (1985).

[53] Parsons, D.K. and Nigg, D.W. "Extension of the Analytic Nodal Method for Four Energy Groups" *Trans. Am. Nuc. Soc.* **50**, 282 (1985).

[54] Larsen, E.W. Private Communication (1998).

[55] Kornreich, D.E., Private Communication (1998,2001).

APPENDIX A
Derivation of One-, Two-, and Three-Group k_∞

To follow the benchmark referenced literature for the multi-group problems, the lowest energy group is group 1. This notation is the reverse from most nuclear engineering textbooks.

I One-Energy Group Infinite Medium k_∞

For an infinite, isotropic, homogeneous medium, the neutron leakage term, $\Omega \cdot \nabla\Psi = 0$, and the angular and scalar neutron flux is constant everywhere. Integrating the one-energy group infinite medium form of the transport equation over angle produces:

$$\Sigma_t\phi = \Sigma_s\phi + \frac{\nu\Sigma_f}{k_\infty}\phi \tag{.1}$$

where ϕ is the scalar neutron flux. The equation can be directly solved for k_∞.

$$k_\infty = \frac{\nu\Sigma_f}{\Sigma_t - \Sigma_s} \tag{.2}$$

or, in terms of mean number of secondaries, c:

$$k_\infty = c\left[\frac{\nu\Sigma_f\Sigma_t}{(\Sigma_t - \Sigma_s)(\Sigma_s + \nu\Sigma_f)}\right] \tag{.3}$$

II Two-Energy Group Infinite Medium k_∞

The two-group infinite medium form of the neutron transport equation reduces to:

$$\Sigma_2\phi_2 = \Sigma_{22s}\phi_2 + \Sigma_{21s}\phi_1 + \frac{\chi_2}{k_\infty}[\nu_2\Sigma_{2f}\phi_2 + \nu_1\Sigma_{1f}\phi_1] \tag{.4}$$

$$\Sigma_1\phi_1 = \Sigma_{11s}\phi_1 + \Sigma_{12s}\phi_2 + \frac{\chi_1}{k_\infty}[\nu_1\Sigma_{1f}\phi_1 + \nu_2\Sigma_{2f}\phi_2] \tag{.5}$$

Rearranging the equations in terms of ϕ_1 and ϕ_2:

$$\left[\Sigma_2 - \Sigma_{22s} - \frac{\chi_2}{k_\infty}\nu_2\Sigma_{2f}\right]\phi_2 - \left[\Sigma_{21s} + \frac{\chi_2}{k_\infty}\nu_1\Sigma_{1f}\right]\phi_1 = 0 \tag{.6}$$

$$\left[\Sigma_1 - \Sigma_{11s} - \frac{\chi_1}{k_\infty}\nu_1\Sigma_{1f}\right]\phi_1 - \left[\Sigma_{12s} + \frac{\chi_1}{k_\infty}\nu_2\Sigma_{2f}\right]\phi_2 = 0 \tag{.7}$$

This equation can be written in matrix form as: [51]

$$\begin{bmatrix} -\left(\Sigma_{21s} + \frac{\chi_2}{k_\infty}\nu_1\Sigma_{1f}\right) & \left(\Sigma_2 - \Sigma_{22s} - \frac{\chi_2}{k_\infty}\nu_2\Sigma_{2f}\right) \\ \left(\Sigma_1 - \Sigma_{11s} - \frac{\chi_1}{k_\infty}\nu_1\Sigma_{1f}\right) & -\left(\Sigma_{12s} + \frac{\chi_1}{k_\infty}\nu_2\Sigma_{2f}\right) \end{bmatrix} \begin{bmatrix} \phi_1 \\ \phi_2 \end{bmatrix} = \begin{bmatrix} 0 \\ 0 \end{bmatrix} \tag{.8}$$

To simplify the matrix elements, it is useful to define a total removal cross section, Σ_g, for each energy group g as the difference between the total cross section and in-group scattering or:[49]

$$\Sigma_2^{rem} = \Sigma_2 - \Sigma_{22s} \tag{.9}$$

$$\Sigma_1^{rem} = \Sigma_1 - \Sigma_{11s} \tag{.10}$$

Setting the determinant of this matrix equal to zero will give an equation that can be solved for k_∞. One solution is $k_\infty = 0$. The other solution is:

$$k_\infty = \frac{\chi_1(\nu_2\Sigma_{2f}\Sigma_{21s} + \Sigma_2^{rem}\nu_1\Sigma_{1f}) + \chi_2(\nu_1\Sigma_{1f}\Sigma_{12s} + \Sigma_1^{rem}\nu_2\Sigma_{2f})}{\Sigma_1^{rem}\Sigma_2^{rem} - \Sigma_{12s}\Sigma_{21s}} \tag{.11}$$

If there is no thermal upscattering, the equation reduces to:

$$k_\infty = \frac{\chi_1\nu_1\Sigma_{1f}}{\Sigma_1^{rem}} + \chi_2\left(\frac{\nu_1\Sigma_{1f}\Sigma_{12s}}{\Sigma_1^{rem}\Sigma_2^{rem}} + \frac{\nu_2\Sigma_{2f}}{\Sigma_2^{rem}}\right) \tag{.12}$$

To obtain the flux ratio, equations 23 and 24 are added to eliminate χ_1 and χ_2 to give:

$$\left[\Sigma_1^{rem} - \Sigma_{21s} - \frac{\nu_1\Sigma_{1f}}{k_\infty}\right]\phi_1 + \left[\Sigma_2^{rem} - \Sigma_{12s} - \frac{\nu_2\Sigma_{2f}}{k_\infty}\right]\phi_2 = 0 \tag{.13}$$

where $\chi_1 + \chi_2 = 1$.

Solving for ϕ_2/ϕ_1:

$$\frac{\phi_2}{\phi_1} = \frac{\left[\Sigma_1^{rem} - \Sigma_{21s} - \frac{\nu_1 \Sigma_{1f}}{k_\infty}\right]}{\left[\frac{\nu_2 \Sigma_{2f}}{k_\infty} - \Sigma_2^{rem} + \Sigma_{12s}\right]} \tag{.14}$$

If there is no thermal upscattering, the equation reduces to:

$$\frac{\phi_2}{\phi_1} = \frac{\left[\Sigma_1^{rem} - \frac{\nu_1 \Sigma_{1f}}{k_\infty}\right]}{\left[\frac{\nu_2 \Sigma_{2f}}{k_\infty} - \Sigma_2^{rem} + \Sigma_{12s}\right]} \tag{.15}$$

III Three-Energy Group Infinite Medium k_∞ (a)

To make the three-energy group problem simpler, the following assumptions are made: [49]

- No thermal upscattering from group j to group i, $j < i$, $\Sigma_{ij_s} = 0$
- No fission neutrons are born in the lowest energy group, i.e. χ_1=0

The neutron transport equation can be written as:

$$\Sigma_3 \phi_3 = \Sigma_{33s}\phi_3 + \frac{\chi_3}{k_\infty}\left[\nu_3\Sigma_{3f}\phi_3 + \nu_2\Sigma_{2f}\phi_2 + \nu_1\Sigma_{1f}\phi_1\right] \tag{.16}$$

$$\Sigma_2 \phi_2 = \Sigma_{22s}\phi_2 + \Sigma_{23s}\phi_3 + \frac{\chi_2}{k_\infty}\left[\nu_3\Sigma_{3f}\phi_3 + \nu_2\Sigma_{2f}\phi_2 + \nu_1\Sigma_{1f}\phi_1\right] \tag{.17}$$

$$\Sigma_1 \phi_1 = \Sigma_{11s}\phi_1 + \Sigma_{12s}\phi_2 + \Sigma_{13s}\phi_2 \tag{.18}$$

Rearranging the equations in terms of ϕ_1, ϕ_2 and ϕ_3:

$$\left[\Sigma_3 - \Sigma_{33s} - \frac{\chi_3}{k_\infty}\nu_3\Sigma_{3f}\right]\phi_3 - \left[\frac{\chi_3}{k_\infty}\nu_2\Sigma_{2f}\right]\phi_2 - \left[\frac{\chi_3}{k_\infty}\nu_1\Sigma_{1f}\right]\phi_1 = 0 \tag{.19}$$

$$-\left[\Sigma_{23s} + \frac{\chi_2}{k_\infty}\nu_3\Sigma_{3f}\right]\phi_3 + \left[\Sigma_2 - \Sigma_{22s} - \frac{\chi_2}{k_\infty}\nu_2\Sigma_{2f}\right]\phi_2 - \left[\frac{\chi_2}{k_\infty}\nu_1\Sigma_{1f}\right]\phi_1 = 0 \tag{.20}$$

$$-\Sigma_{13s}\phi_3 - \Sigma_{12s}\phi_2 + \left[\Sigma_1 - \Sigma_{11s}\right]\phi_1 = 0 \tag{.21}$$

This equation can be written in matrix form as: [49]

$$\begin{bmatrix} \left(\Sigma_3 - \Sigma_{33s} - \frac{\chi_3}{k_\infty}\nu_3\Sigma_{3f}\right) & -\left(\frac{\chi_3}{k_\infty}\nu_2\Sigma_{2f}\right) & -\left(\frac{\chi_3}{k_\infty}\nu_1\Sigma_{1f}\right) \\ -\left(\Sigma_{23s} + \frac{\chi_2}{k_\infty}\nu_3\Sigma_{3f}\right) & \left(\Sigma_2 - \Sigma_{22s} - \frac{\chi_2}{k_\infty}\nu_2\Sigma_{2f}\right) & -\left(\frac{\chi_2}{k_\infty}\nu_1\Sigma_{1f}\right) \\ -\Sigma_{13s} & -\Sigma_{12s} & (\Sigma_1 - \Sigma_{11s}) \end{bmatrix} \begin{bmatrix} \phi_1 \\ \phi_2 \\ \phi_3 \end{bmatrix} = \begin{bmatrix} 0 \\ 0 \\ 0 \end{bmatrix} \tag{.22}$$

Using the total removal cross sections defined in equations 26 and 27, the determinant of the matrix then becomes:

$$\begin{bmatrix} \left(\Sigma_3^{rem} - \frac{\chi_3}{k_\infty}\nu_3\Sigma_{3f}\right) & -\left(\frac{\chi_3}{k_\infty}\nu_2\Sigma_{2f}\right) & -\left(\frac{\chi_3}{k_\infty}\nu_1\Sigma_{1f}\right) \\ -\left(\Sigma_{23s} + \frac{\chi_2}{k_\infty}\nu_3\Sigma_{3f}\right) & \left(\Sigma_2^{rem} - \frac{\chi_2}{k_\infty}\nu_2\Sigma_{2f}\right) & -\left(\frac{\chi_2}{k_\infty}\nu_1\Sigma_{1f}\right) \\ -\Sigma_{13s} & -\Sigma_{12s} & \Sigma_1^{rem} \end{bmatrix} \tag{.23}$$

If we multiply the second line by χ_3, multiply the first line by χ_2, and subtract the results, and multiply the first line by k_∞, the determinant becomes:

$$\begin{bmatrix} (\Sigma_3^{rem}k_\infty - \chi_3\nu_3\Sigma_{3f}) & -(\chi_3\nu_2\Sigma_{2f}) & -(\chi_3\nu_1\Sigma_{1f}) \\ -(\chi_3\Sigma_{23s} + \chi_2\Sigma_3^{rem}) & (\chi_3\Sigma_2^{rem}) & 0 \\ -\Sigma_{13s} & -\Sigma_{12s} & \Sigma_1^{rem} \end{bmatrix} \tag{.24}$$

Two of the k_∞ solutions are zero. The other solution is:

$$k_\infty = \frac{(\chi_3\Sigma_{23s} + \chi_2\Sigma_3^{rem})(\nu_1\Sigma_{1f}\Sigma_{12s} + \nu_2\Sigma_{2f}\Sigma_1^{rem}) + \chi_3\Sigma_2^{rem}(\nu_1\Sigma_{1f}\Sigma_{13s} + \nu_3\Sigma_{3f}\Sigma_1^{rem})}{\Sigma_1^{rem}\Sigma_2^{rem}\Sigma_3^{rem}} \tag{.25}$$

IV Three-Energy Group Infinite Medium k_∞ (b)

An alternative method for solving the three-group k_∞ problem [47] is to rearrange the three-group transport equations in equations 33, 34, 35:

$$(\Sigma_3 - \Sigma_{33s})\,\phi_3 = \frac{\chi_3}{k_\infty}\left[\nu_3\Sigma_{3f}\phi_3 + \nu_2\Sigma_{2f}\phi_2 + \nu_1\Sigma_{1f}\phi_1\right] \tag{.26}$$

$$(\Sigma_2 - \Sigma_{22s})\,\phi_2 = \Sigma_{23s}\phi_3 + \frac{\chi_2}{k_\infty}\left[\nu_3\Sigma_{3f}\phi_3 + \nu_2\Sigma_{2f}\phi_2 + \nu_1\Sigma_{1f}\phi_1\right] \tag{.27}$$

$$(\Sigma_1 - \Sigma_{11s})\,\phi_1 = \Sigma_{12s}\phi_2 + \Sigma_{13s}\phi_3 \tag{.28}$$

Divide each equation by ϕ_3 and define:

$$\phi_{23} = \frac{\phi_2}{\phi_3} \tag{.29}$$

$$\phi_{13} = \frac{\phi_1}{\phi_3} \tag{.30}$$

$$\Sigma_i^{rem} = \Sigma_i - \Sigma_{iis} \tag{.31}$$

The result gives:

$$\Sigma_3^{rem} = \frac{\chi_3}{k_\infty}\left[\nu_3\Sigma_{3f} + \nu_2\Sigma_{2f}\phi_{23} + \nu_1\Sigma_{1f}\phi_{13}\right] \tag{.32}$$

$$\phi_{23}\Sigma_2^{rem} = \Sigma_{23s} + \frac{\chi_2}{k_\infty}\left[\nu_3\Sigma_{3f} + \nu_2\Sigma_{2f}\phi_{23} + \nu_1\Sigma_{1f}\phi_{13}\right] \tag{.33}$$

$$\phi_{13}\Sigma_1^{rem} = \Sigma_{13s} + \Sigma_{12s}\phi_{23} \tag{.34}$$

If we divide equations 50 and 51 by $\nu_3\Sigma_{3f}$ and define:

$$f_{23} = \frac{\nu_2\Sigma_{2f}}{\nu_3\Sigma_{3f}}\phi_{23} \tag{.35}$$

$$f_{13} = \frac{\nu_1\Sigma_{1f}}{\nu_3\Sigma_{3f}}\phi_{13} \tag{.36}$$

Then we get:

$$\frac{\Sigma_3^{rem}}{\chi_3\nu_3\Sigma_{3f}} = \frac{1}{k_\infty}\left[1 + f_{23} + f_{13}\right] \tag{.37}$$

$$\frac{1}{\chi_2\nu_3\Sigma_{3f}}\left[\Sigma_2^{rem}\phi_{23} - \Sigma_{23s}\right] = \frac{1}{k_\infty}\left[1 + f_{23} + f_{13}\right] \tag{.38}$$

$$\phi_{13}\Sigma_1^{rem} = \Sigma_{13s} + \Sigma_{12s}\phi_{23} \tag{.39}$$

If we substitute equation 56 into 57 and rearranging,

$$\frac{\Sigma_2^{rem}}{\Sigma_3^{rem}}\phi_{23} = \frac{\Sigma_{23s}}{\Sigma_3^{rem}} + \frac{\chi_2}{\chi_3} \tag{.40}$$

$$\frac{\Sigma_1^{rem}}{\Sigma_3^{rem}}\phi_{13} = \frac{\Sigma_{13s}}{\Sigma_3^{rem}} + \frac{\Sigma_{12s}}{\Sigma_3^{rem}}\phi_{23} \tag{.41}$$

$$k_\infty = \frac{\chi_3\nu_3\Sigma_{3f}}{\Sigma_3^{rem}}\left[1 + f_{23} + f_{13}\right] \tag{.42}$$

Equations 57, 58, and 59 give the flux ratios and k_∞. Tables 43, 44, and 45 give the cross sections used for the three-group problem.[47]

There are numerous cross sections involved in these equations, implying that there are numerous arbitrary choices we can make that will yield solutions to these equations. We show **one** set of cross sections that will satisfy a set of chosen conditions.[47]

If we make our basic choices as:

- $k_\infty = 1.600$
- χ_3=0.96, χ_2=0.04, χ_1=0.0
- 5% of fission production occurs in group 3
- 20% of fission production occurs in group 2
- 75% of fission production occurs in group 1

With these choices and the definitions of f_{23} and f_{13}, we get:

$$f_{23} = \frac{\nu_2 \Sigma_{2f}}{\nu_3 \Sigma_{3f}} \frac{\phi_2}{\phi_3} = 4 \tag{.43}$$

$$f_{13} = \frac{\nu_1 \Sigma_{1f}}{\nu_3 \Sigma_{3f}} \frac{\phi_1}{\phi_3} = 15 \tag{.44}$$

Using this gives:

$$\frac{\Sigma_3^{rem}}{\nu_3 \Sigma_{3f}} = \frac{\chi_3}{k_\infty} [1 + f_{23} + f_{13}] \tag{.45}$$

$$\frac{\Sigma_3^{rem}}{\nu_3 \Sigma_{3f}} = 12.0 \tag{.46}$$

We can now make more arbitrary choices. If we choose:

- ν_3=3.0, Σ_{3f}=0.006
- ν_2=2.5, Σ_{2f}=0.060
- ν_1=2.0, Σ_{1f}=0.900

Then we get:

$$\phi_{23} = 0.480 \tag{.47}$$

$$\phi_{13} = 0.150 \tag{.48}$$

making Σ_3^{rem}=0.216 from equation 63. If we make more choices:

$$\Sigma_{33s} = 0.024 \tag{.49}$$

$$\Sigma_{3c} = 0.006 \tag{.50}$$

$$\Sigma_{13s} = 0.033 \tag{.51}$$

making Σ_3=0.240 and Σ_{23s}=0.171. Using equation 57, Σ_2^{rem}=0.375. This result now gives:

$$\Sigma_{22s} = 0.600 \tag{.52}$$

$$\Sigma_{2c} = 0.040 \tag{.53}$$

making Σ_2=0.975 and Σ_{12s}=0.275. Using equation 58, Σ_1^{rem}=1.10. One last arbitrary choice is:

$$\Sigma_{11s} = 2.00 \tag{.54}$$

making Σ_1=3.10 and Σ_{1c}=0.20.

V *General Multigroup Infinite Medium* k_∞

More than three-group k_∞ derivations have been done (see reference [53]). A general multigroup k_∞ derivation is included in this section for completeness.[54]

Given

$$\overline{\overline{\Sigma_t}}\ \overline{\phi} = \overline{\overline{\Sigma_s}}\ \overline{\phi} + \frac{\overline{\chi}\ \overline{\nu\Sigma_f}\ \overline{\phi}}{k} \tag{.55}$$

where:

$\overline{\overline{\Sigma_t}} = GxG$ matrix
$\overline{\overline{\Sigma_s}} = GxG$ matrix
$\overline{\chi} = Gx1$ vector
$\overline{\nu\Sigma_f} = 1xG$ vector
$\overline{\phi} = Gx1$ vector
$k =$ scalar

then:

$$\left(\overline{\overline{\Sigma_t}} - \overline{\overline{\Sigma_s}}\right)\ \overline{\phi} = \frac{1}{k}\overline{\chi}\ \overline{\nu\Sigma_f}\ \overline{\phi} \tag{.56}$$

$$\overline{\phi} = \frac{1}{k}\left(\overline{\overline{\Sigma_t}} - \overline{\overline{\Sigma_s}}\right)^{-1}\overline{\chi}\ \overline{\nu\Sigma_f}\ \overline{\phi} \tag{.57}$$

$$\overline{\nu\Sigma_f}\ \overline{\phi} = \frac{1}{k}\overline{\nu\Sigma_f}\left(\overline{\overline{\Sigma_t}} - \overline{\overline{\Sigma_s}}\right)^{-1}\overline{\chi}\ \overline{\nu\Sigma_f}\ \overline{\phi} \tag{.58}$$

Since $\nu\Sigma_f\phi$ is a scalar, it can be cancelled out and we get the followng explicit result:

$$k = \overline{\nu\Sigma_f}\left(\overline{\overline{\Sigma_t}} - \overline{\overline{\Sigma_s}}\right)^{-1} \overline{\chi} \tag{.59}$$

The right hand side of this equation is a scalar, equal to k. Only one matrix inversion is necessary.